https://doi.org/10.5194/egusphere-2026-4047
Preprint. Discussion started: 20 August 2026

Changes in temperature sensitivity of soil respiration with decadal warming

Linsey Maria Avila[1], Jesper Riis Christiansen[1], Bjarni Diðrik Sigurdsson[2], and Klaus Steenberg Larsen[1]

[1]Department of Geosciences & Natural Resource Management, University of Copenhagen, Denmark
[2]Faculty of Environmental & Forest Sciences, Agricultural University of Iceland, Iceland

Correspondence to: ksl@ign.ku.dk | +45 35 33 76 54

Abstract. Global warming may enhance soil organic carbon (*SOC*) turnover and CO_2 release, potentially accelerating further warming in a positive feedback loop. The temperature sensitivity (*TS*) of soil respiration is a key determinant for the climate feedback of soils. However, it is uncertain how *TS* may change under continued warming due to potential microbial thermal acclimation and changes in substrate quality and availability. We examined *TS* in an incubation experiment using intact soil cores that had undergone 13 years (decadal) of *in situ* geothermal warming spanning a broad warming gradient of +0 °C to +75 °C.

The observed loss of *SOC* stock (medians ± SE, kg C m^{-2}) compared to ambient had increased with decadal warming, from -4.9 ± 2.4% at +1–3 °C to -19.3 ± 1.5% at +7–10 °C. Across incubation temperatures from 5 to 35 °C in the lab experiment, area-based *TS* generally declined with decadal warming intensity while *SOC*-normalized *TS* was similar across treatments. This suggests that *SOC* depletion rather than microbial thermal acclimation was the dominant control for reduced respiration rates with warming. *TS* showed variation with temperature range and was generally lower between the 5–15 °C and 25–35 °C incubation temperature changes and markedly higher in the 15–25 °C change. Best-fit standard field models for soil respiration (Van't Hoff and Lloyd & Taylor models, R^2 = 0.842–0.929) failed to capture these shifts in *TS*, while a sigmoidal function closely captured the observed *TS* dynamics (R^2 = 0.970–0.998). Our study suggests that using fixed Q_{10} *TS* values to upscale C budgets is inadequate. Although area-based respiration rates declined with warming, the observed decline in soil respiration with warming suggests a latent reduction of further *SOC* loss over time following prolonged exposure to warming.

1 Introduction

Understanding the response of soil organic carbon (*SOC*) pools to warming is important for predicting soil-atmosphere feedback mechanisms in a future warmer climate. This is especially important for high-latitude terrestrial soils on the northern hemisphere (above 60°N), which contain over 400 Gt C or about a fourth of global *SOC* to a 1 m depth (Ito et al., 2016). In the past decades alone, these regions have experienced double the warming than the rest of the world (IPCC, 2022). Extreme warming events, such as the winters of 2016 and 2018, when polar region surface temperatures rose 6°C above the previous decade (IPCC, 2023), are also projected to become more frequent in a future, warmer world. As temperatures rise more

https://doi.org/10.5194/egusphere-2026-4047
Preprint. Discussion started: 20 August 2026

drastically and recurrently in the Arctic and subarctic, there is a potential for larger effects on *SOC* pools within these regions. Recent global syntheses show that *SOC* losses due to warming are most pronounced in high-latitude regions, where large initial *SOC* stocks and rapid temperature increases make these ecosystems particularly vulnerable to accelerated C loss (Crowther et al., 2016).

While strong soil warming can lead to rapid net loss of *SOC* within a few years (Poeplau et al., 2017; Poeplau et al., 2020; Verbrigghe et al., 2022) indicating a strong, apparent *TS*, it is largely unknown how *SOC* pools in high latitude mineral soils respond to warming over decades. It is also unclear whether the *TS* of soil respiration is maintained or altered as *SOC* pools develop and soil microbial communities potentially acclimate within these decadal timescales. Here, we use the term thermal acclimation to describe any decline in the *TS* of soil respiration under prolonged warming not attributed to substrate depletion, without assuming specific physiological or community-level mechanisms (Tucker et al., 2013; Alster et al., 2023; Qu et al., 2024; Sun et al., 2023). However, decadal or long-term warming manipulation experiments that go beyond 5 years are rare and the experimental warming in such experiments typically never exceeds more than a maximum of 6°C above ambient (Ziegler et al., 2017; Li et al., 2024; Du et al., 2023; Liang et al., 2024).

Empirical studies from geothermal gradient systems show that microbial activity remains intrinsically temperature-sensitive even after decades of warming, but that sustained C loss eventually leads to substrate depletion, which constrains microbial biomass and respiration (Walker et al., 2018; Melillo et al., 2017). On the other hand, other studies have observed evidence of microbial thermal acclimation over time, where respiration rates decline relative to initial responses under prolonged warming (Li et al., 2023; Crowther and Bradford, 2013; Cruz-Paredes et al., 2023). Together, these findings suggest that long-term warming effects on soil respiration may be shaped by both reductions in substrate availability and shifts in microbial *TS*.

Predicting the warming effect on *SOC* turnover by enhanced heterotrophic respiration has often relied on applying a single, universal modeled *TS* constant (Q_{10}) (von Lützow and Kögel-Knabner, 2009; Foereid et al., 2014; Meyer et al., 2018). Deriving Q_{10} in this way is typically based on temperature response functions such as Van't Hoff (1900) or other Arrhenius-derived equations (Robinson et al., 2017; Čapek et al., 2019; Azizi-Rad et al., 2022; Numa et al., 2021), assuming that a static Q_{10} applies uniformly across temperature ranges and time. Other response functions, like the Lloyd and Taylor (1994) model, allow for slight flexibility in *TS*. Many Earth system models that assume universal *TS* fail to capture the adaptive behavior of these processes, potentially misrepresenting future C balance projections (Cruz-Paredes et al., 2023). While seasonally varying *TS* for soil and ecosystem respiration have been incorporated into ecosystem-scale models (Torn et al., 2025), these efforts often focus on intra-annual variability (e.g. seasonal temperature shifts). Such approaches may reflect short-term systemic changes. However, they do not account for the potential changes in turnover rates over temporal scales relevant to observed climate warming (e.g. decades), nor do they fully incorporate variation across a broad range of different warming intensities.

https://doi.org/10.5194/egusphere-2026-4047
Preprint. Discussion started: 20 August 2026

To reconcile this knowledge, gap the major objective of this study was to investigate how the *TS* of soil respiration was impacted by the combined effects of short-term warming (5, 15, 25, and 35 °C) and decadal soil warming at multiple levels along a large geothermal gradient (+0 to +75°C). The uniquely large decadal warming gradient used enabled an analysis of potential thresholds for changes in temperature sensitivities in underlying processes (O'Gorman et al., 2021). We hypothesized that the *TS* of soil respiration over our broad warming range would be dampened with increasing decadal warming level due to a depletion of *SOC* coupled with thermal acclimation.

To test the hypothesis, we incubated intact soil cores from a unique natural soil warming site in Iceland. We sampled mineral Andosols exposed to warming along a naturally occurring soil temperature gradient that was created after an earthquake 13 years ago, spanning from +0 to +75°C of decadal warming above ambient. With this experiment, we go beyond the typical +1 to +3 °C used in most previous climate-warming manipulation experiments. This extended gradient enabled us to identify whether thresholds or shifts in *SOC* responses to warming exist at higher, less-studied temperatures, with the goal of expanding our understanding of *SOC* loss and potential soil microbial thermal acclimation over decadal time scales.

2 Materials & Methods

2.1 Study site description

Located in southern Iceland, adjacent to the village of Hveragerði, the study site (64.007°N, 21.175°W, 83-168m a.s.l.) lies within one of the two "ForHot" grassland experimental field sites (Sigurdsson et al., 2016). A 6.3 magnitude earthquake in May of 2008 (Halldórsson and Sigbjörnsson, 2009) created a new geothermal hotspot within the bedrock under the unmanaged grassland ecosystem at the site (termed the "Medium-Term Warmed" site, MTW, in earlier studies, e.g. N. Verbrigghe et al. (2022). At the time of sampling the soil had been warmed for ~13 years, which we therefore here term "decadal warming".

The whole mineral soil profile is warmed by thermal diffusion from the bedrock, creating an area around the hotspot where soil temperatures at 10 cm depth ranged from +75°C at the center to no warming (+0°C) ~60m away. The climate at the site is subarctic and characterized by high and prolonged periods of precipitation with naturally short growing seasons ranging from 90 to 130 days, typically starting in May and ending in August. For the year the incubation samples were collected (2021), the mean annual air temperature (MAT), measured at 0.75 m above the ground surface, and mean volumetric soil water content (SWC), measured at 5 cm below the ground surface, at the field site were 7.3°C and 25.5%, respectively. The total annual precipitation measured was 1415 mm at the closest Icelandic Meteorological Office (2024) synoptic station in Hjarðarland, 35 km from the site. Within the soil sampling period (September 30 to October 2, 2021), the mean air temperature was 6.6°C and the mean SWC was 29.0% while total precipitation for September and October 2021 were 206 and 72 mm, respectively.

The vegetation is dominated by *Agrostis capillaris* (Sigurdsson et al., 2016) with a mix of other monocot and dicot species, *Anthoxantum odoratum, Poa pratensis*, *Carex nigra*, *Gallium boreale*, *Ranunculus acris* and mosses up to ca. +20°C warming

https://doi.org/10.5194/egusphere-2026-4047
Preprint. Discussion started: 20 August 2026

(Loock, 2017; Kristinsson, 2010) and thereafter mostly by mosses only as the soil in the rooting zone becomes too warm for most of the vascular plants. Due to the decadal soil warming, there have been shifts in length and variability of the growing season. In ambient plots, the typical growing season length for the region is still present, while plots exposed to warming of 7-10°C above ambient have both an earlier start and later end of the growing season, extending it by more than 40 days beyond the typical 90-130 days (Leblans et al., 2017; Mortier et al., 2024).

The soil type at this site is Brown Andosols, which is comprised of volcanic particulate with a silty loam texture. It possess relatively high clay content which is dominated by allophane and ferrihydrite, Al/Fe-humus complexes, which give these soils a rather low bulk density, high water holding capacity and, thus, hydraulic conductivity (Arnalds, 2015; Johannesson, 1960). During the non-growing season, the topsoil in unwarmed (+0°C) and low-level warming (+1-3°C) plots may freeze for a couple of months in the winter with sporadic periods of persistent snow cover usually taking place in late winter and early spring (Sigurdsson et al., 2016). The soil depth at the site is generally shallow, ranging from a maximum of 54.1 cm in the ambient permanent plots to a minimum of 27.4 cm in the high-warming permanent plots (Sigurdsson et al., 2016). Several of our sampled plots also had soil depths < 25 cm, particularly those closest to the geothermal hotspot.

2.2 Sample selection & collection

Soil sampling was done from September 30 to October 2, 2021. Within 60 m of the geothermal hotspot, 70 soils samples at 14 individual sampling locations were collected along a geothermal soil temperature (T_{soil}) gradient (Figure 1). At each sampling location five replicates were collected within 10 centimeters of each other. We classified 6 decadal warming levels with average T_{soil} ranges of ambient (+0°C above ambient, i.e. no warming), low (+1 to 3°C above ambient), mid (+7 to 10°C above ambient), mid-high (+15 to 20°C above ambient), high (+25 to 35°C above ambient), and the geothermal hotspot (+75°C above ambient) based on the permanent plot classification described by Sigurdsson et al. (2016). Due to space limitations at the site and to avoid disturbing permanent sampling plots, 3 sampling locations were available for the ambient, low, and mid warming levels, while only 2 sampling locations were available for the mid-high, and high levels, and only one sampling location was available for the geothermal hotspot.

https://doi.org/10.5194/egusphere-2026-4047
Preprint. Discussion started: 20 August 2026

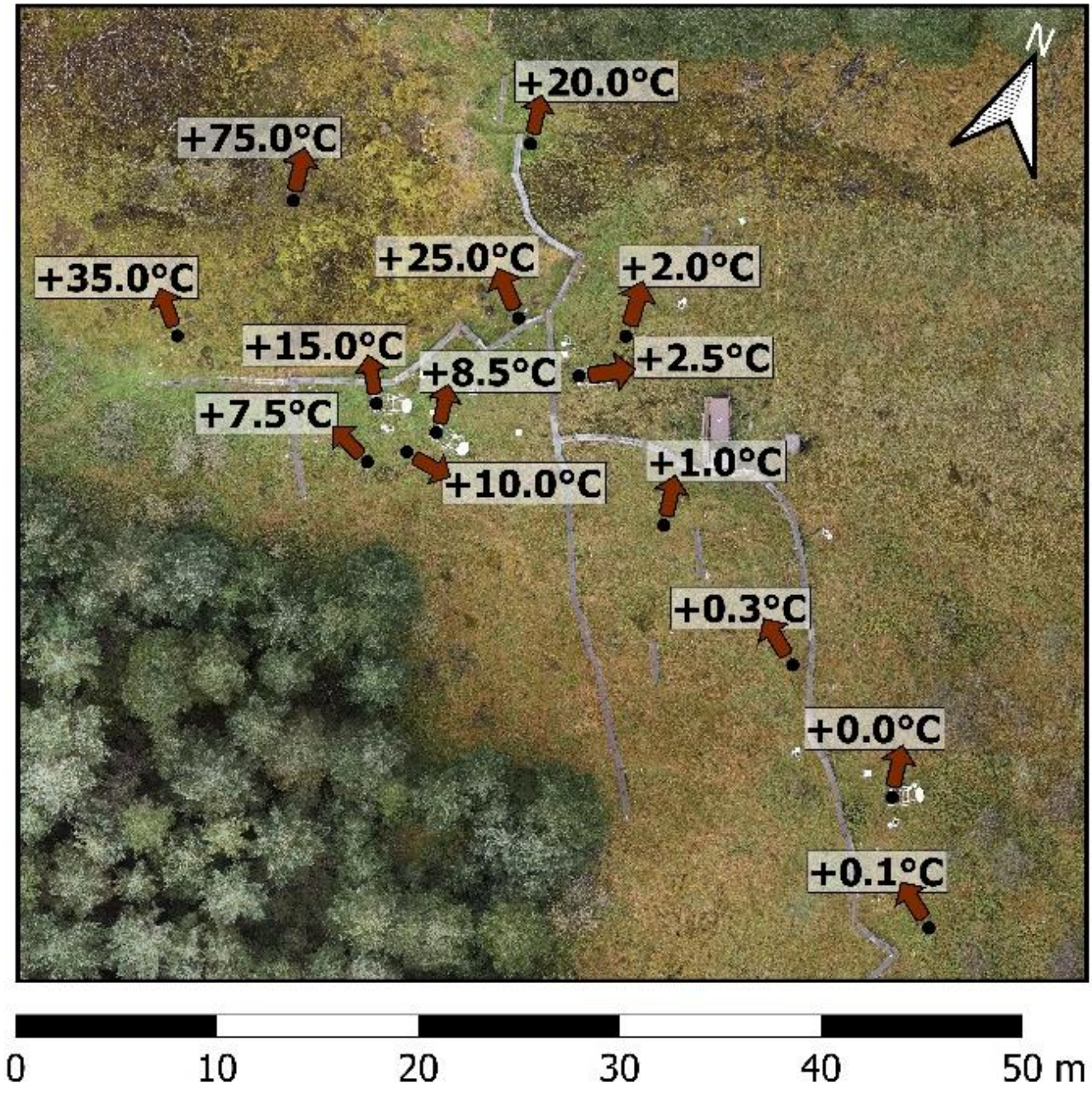

Figure 1. Aerial view of the study site with the 14 decadal warming sampling locations displayed with the temperature increase for each compared to control plotted in the computer program QGIS (version 3.34) using an orthomosaic composite created by Amir Hamedpour (2021) from a series of unmanned aerial vehicle (UAV) images in bands red, blue, green (RBG) at a spatial resolution of 5 mm

https://doi.org/10.5194/egusphere-2026-4047
Preprint. Discussion started: 20 August 2026

Incubation soil core rings with a height of 3.5 cm and a diameter of 6 cm were used to excavate each soil sample as intact as possible from the topsoil layer. This 3.5 cm section was chosen because it isolates the biologically active horizon most responsive to warming (Wasner et al., 2025; Sun et al., 2025). It also provides a consistent sampling depth across plots, which is essential for comparable *SOC* and bulk-density measurements (FAO, 2020; Crowther et al., 2016; Poeplau et al., 2018). Because the soil profile at this site is shallow and Icelandic Andosols typically have limited vertical development (Arnalds, 2015), maintaining a uniform sampling depth is especially important.

Before extracting the soil cores, all aboveground vegetation within the 6 cm ring area was clipped at the soil surface and placed in 20 × 25 cm paper bags for later biomass assessment. After fieldwork, soil cores and aboveground vegetation was weighed to ensure field capacity weights could be maintained during later soil core incubations. The vegetation bags were then oven-dried at 55 °C for at least 96 h and then weighed again to obtain dry mass. During core extraction, roots protruding outside of the base of the core sample were trimmed so that only material contained within the intact core (i.e., roots and soil) was retained. The soil samples were taken from a soil depth of 5 (± 0.5) cm below the soil surface, thus covering the topsoil layer only. Directly following extraction, the intact soil cores were wrapped in plastic film and sealed with adhesive tape to maintain soil structure, and were stored at 4 °C to induce dormancy until the start of the incubation experiment three months later.

2.3 Temperature sensitivity incubation experiment

The investigation of *TS* of soil respiration, incubated between 5–35 °C in increments of 10 °C, was based on the intact soil core method to minimize disturbance of the soil structure that otherwise can bias results (Kan et al., 2022). Before starting the experiment, all samples were water saturated with millipore deionized water and then drained to field capacity. They were then transferred to 0.35 L glass jars and covered with parafilm to minimize water loss during a pre-incubation period of 24 h at 5 °C. During the pre-incubation and incubation periods, all of the samples were stored in a temperature-controlled climate chamber (± 0.1 °C from target temperature), which was flushed continuously with outdoor, ambient air at a rate of 100 L min^{-1} to avoid a build-up of the CO_2 concentration inside the chamber prior to measurements that could in turn lead to erroneous fluxes upon measuring. All samples were exposed to a stepwise incubation scheme with a maximum of 24 h for incubation at each temperature step (5 °C, 15 °C, 25 °C, and 35 °C) to minimize the potential confounding effect of the natural loss of *SOC* over an extended period of incubation time. Gas flux measurements were always performed at least 12 h after the start of each temperature step to ensure that the whole sample had reached the incubation temperature. At the end of each incubation step, samples were weighed and deionized water was added to samples where water loss occurred to bring them back to field capacity in preparation for the next incubation step.

During gas flux measurements, the jars containing the intact soil cores were transferred to a water bath maintained at the incubation temperature (± 0.8 °C). The parafilm cover was then replaced with customized lids fitted with tubing to pre-flush the samples with ambient outdoor air (400–440 ppm CO_2) for a minimum of 7 min at a flow rate of 4 L min^{-1} prior to each flux

https://doi.org/10.5194/egusphere-2026-4047
Preprint. Discussion started: 20 August 2026

measurement. The CO_2 concentration of the intake air from the flush line was monitored between measurements to ensure it remained within this ambient range (≤ 440 ppm CO_2) before initiating the pre-flush, following established protocols recommending equilibration with ambient air prior to measurement (Parkin and Venterea, 2010; Pumpanen et al., 2004; Jian et al., 2021). Given that mean atmospheric CO_2 during the experimental period was assumed to be ~420 ppm, this range should have adequately reflected normal variability, with ambient CO_2 typically fluctuating by ± 20–30 ppm around the mean depending on local atmospheric mixing and seasonal dynamics (NOAA, 2024). Thus, flux measurement concentrations at time zero kept within this ambient range would not have created an artificial soil–headspace CO_2 gradient large enough to influence diffusion beyond real-world atmospheric conditions (Fang and Moncrieff, 2001; Phillips et al., 2017; Bond-Lamberty et al., 2018). Therefore, we can be confident that our pre-flush procedure produced a natural, steady-state soil–headspace gradient prior to each measurement (Maier et al., 2022).

The gas flux measurements were performed by switching from the pre-flushing loop to the measurement loop (air flow 0.5 L min^{-1}) where the CO_2 dry fraction concentration was measured at 1 Hz by an LGR-ICOS Microportable Greenhouse Gas Analyzer (GLA131-GGA, LGR-ABB, Canada) for a measurement period of 180 s. The analyzer was also flushed with ambient air for a minimum of 30 s prior to flux measurement. All 70 soil samples at each incubation temperature were measured within the 12-hour period with samples randomized to safeguard against temporal bias between treatments (Boyd et al., 2022). Flux measurements where technical errors were observed (e.g. too high initial CO_2 concentration or non-steady pattern of CO_2 increase over time) were re-measured at the end of each incubation period so that erroneous measurements could later be replaced during data analysis. This was the case for a total of 48 measurements (i.e. 14.6 % of the samples) over all four temperature incubation steps.

2.4 Laboratory SOC, soil, and vegetation analysis

Once the incubation flux measurements were completed, the intact sore soil cores were sieved at a coarseness of two mm to separate the roots, stones (> 2 mm), and soil particulates (< 2 mm). The rocks, roots, and soil were then weighed, and the separated roots and soil were then placed in an oven at 55°C for two weeks after which dry weights were obtained and all sample fractions of soil, roots, stones, and water could be calculated (Figure S1). A sub-sample of sieved dry soil (3 g) from each sample was milled using a Planetary Ball Mill PM 400 (RETSCH, Germany) for subsequent *SOC* concentration examination (%C). 50 mg of milled soil per sample was extracted for the *SOC* concentration analysis, which was performed using a FlashEA Nitrogen and Carbon analyzer (Thermo Scientific, Denmark) under the standard combustion process. Dry soil bulk density (ρ_{bulk}; g cm^{-3}), using the corrected sample core volume (cm^3), was calculated in Eq. 1:

$$\rho_{bulk} = \frac{m_{dry\ soil}}{V_{core} - \left(\frac{m_{stone}}{\rho_{stone}} + \frac{m_{root}}{\rho_{root}}\right)} \quad (1)$$

https://doi.org/10.5194/egusphere-2026-4047
Preprint. Discussion started: 20 August 2026

where $m_{dry\ soil}$ is the dry soil mass in the sample in g, V_{core} is the total volume of the soil sample core in cm³, m_{stone} is the stone mass in the sample in g, ρ_{stone} is the stone density in g cm^{-3}, m_{root} is the fresh root mass in the sample in g, ρ_{root} is the fresh root density in g cm^{-3}. We used a ρ_{stone} of 2.2 g cm^{-3} for vesicular basalt clasts typical of the area (Scott et al., 2023; Franzson et al., 2010; Thien et al., 2015) and ρ_{root} of 1.0 g cm^{-3} for fresh roots (Taseski et al., 2021).Topsoil *SOC* stock (g C cm^{-2}) was then determined by correcting *SOC* concentration (% C) by converting it to g C 100 g dry soil^{-1} and then multiplying by ρ_{bulk} (g cm^{-3}) and the fixed sample height (3.5 cm). *SOC* stock was then converted to kg C m^{-2} to be more readily comparable to both area-based fluxes and vegetation biomass stock with the areal unit of m^{-2}.

The resulting metrics were *SOC* concentration (% C), dry soil bulk density (ρ_{bulk}; g cm^{-3}), *SOC* stock (kg C m^{-2}), and vegetation biomass stock (kg m^{-2}), each with standard error (±SE) from the median. A Kruskal–Wallis rank sum omnibus test, with five degrees of freedom, was performed to test for differences between decadal warming levels within these metrics using the "kruskal.test" function in the stats package (version 4.4.2) from R Core Team (2025). When a significant Kruskal–Wallis result was found, Dunn's post hoc test for multiple comparisons was applied using the "dunnTest" function from the FSA package (version 0.9.6; Ogle et al., 2025) in R Core Team (2025), with *p*-values adjusted using the Holm method to control the family-wise error rate. This procedure outputs adjusted *p*-values and standardized Z-statistics for each pairwise comparison, enabling assignment of compact letter displays for group separation in subsequent visualizations.

2.5 Respiration analysis & empirical modeling

In total, 328 flux measurements were performed, where the duplicate measurement with most linear extent and with the initial CO_2 concentration closest to ambient was chosen. A total of 48 duplicate measurements were excluded in this process. Before data analysis, an additional 6 measurements (2.1% of 280 remaining measurements) were identified as erroneous based on high starting CO_2 concentrations during flux measurement (i.e., > 9% above ambient) and values falling more than two standard deviations from the mean within each decadal warming level. This left a total of 274 measurements to be included in further data analysis.

To estimate the CO_2 flux, linear regression models were fit to the measured dry air concentration of CO_2 (C_{dry}) over time (t) for each incubation measurement, using a fixed deadband of 30 seconds, i.e. leaving a time window of 150 s for the model fit. These were preformed using the AICcmodavg package (version 2.3.3; Mazerolle, 2023) in R Core Team (2025). The fluxes by sample area (F_A) in µmol CO_2 m^{-2} s^{-1} were calculated as follows:

$$F_A = \frac{\Delta C_{dry}}{\Delta t} \cdot \frac{V_{total} \cdot \left[P \cdot \left(1 - \frac{W}{1000}\right)\right]}{R \cdot (273.15 + T_{chamber})} \cdot \frac{1}{A} \quad (2)$$

where $\frac{\Delta C_{dry}}{\Delta t}$ is the slope in ppm CO_2 s^{-1} of the linear regression. V_{total} is the total volume of the sample chamber, tubing, and gas analyzer in L, P is air pressure in atmosphere (atm), W is the water vapor concentration in mmol H_2O mol^{-1} air at time

https://doi.org/10.5194/egusphere-2026-4047
Preprint. Discussion started: 20 August 2026

zero to account for the water vapor pressure, R is the universal gas constant (0.08206 L atm K^{-1} mol^{-1}), $T_{chamber}$ is the air temperature inside the sample chamber in °C, and A is the soil sample area in m^2.

Fluxes were also calculated per g dry soil (F_S) in µg CO_2-C g $soil^{-1}$ h^{-1} and per g SOC (F_C) in µg CO_2-C g SOC^{-1} h^{-1} using Eq.. 3 and 4, respectively:

$$F_S = \frac{\Delta C_{dry}}{\Delta t} \cdot \frac{V_{total} \cdot \left[P \cdot \left(1 - \frac{W}{1000}\right)\right]}{R \cdot (273.15 + T_{chamber})} \cdot \frac{3600 \cdot 12.01}{m_{dry\ soil}} \quad (3)$$

$$F_C = \frac{\Delta C_{dry}}{\Delta t} \cdot \frac{V_{total} \cdot \left[P \cdot \left(1 - \frac{W}{1000}\right)\right]}{R \cdot (273.15 + T_{chamber})} \cdot \frac{3600 \cdot 12.01}{m_{dry\ soil} \cdot SOC} \quad (4)$$

where 3600 is the conversion from seconds to hours, 12.01 is the molar weight of C, and SOC is the weight fraction of the organic carbon to $m_{dry\ soil}$.

Because each incubation step differed by 10 ºC, observed TS (TS_o) values for soil respiration, using the actual Q_{10} formula, were calculated directly from the observed F_A fluxes from Eq. 2 using Eq. 5 for the three incubation temperature intervals of 5 to 15ºC, 15 to 25ºC, and 25 to 35ºC:

$$TS_o = \left(\frac{observed\ R_{s2}}{observed\ R_{s1}}\right)^{\left(\frac{10}{T_2 - T_1}\right)} \quad (5)$$

where $observed\ R_{s1}$ and $observed\ R_{s2}$ are the measured soil respiration rates (F_A) at the lower (T_1) and higher (T_2) incubation temperatures, respectively. Since the difference between $T_2 - T_1 = 10$ in our incubations, Eq. 5 can simply be reduced to $observed\ R_{s2}$ / $observed R_{s1}$. Because TS_o is calculated on a per-sample basis over a 10 °C step, SOC normalization would cancel out and yield identical values to those of our area-based fluxes; therefore, we only report TS_o from area-based fluxes, using SOC-normalized modeling separately to assess SOC effects on the temperature response across decadal warming levels.

Temperature responses using the respiration rates of all four incubation temperature steps were modeled using Van't Hoff (1898) and Lloyd-Taylor (1994) functions shown in Eq. 6 and 7, respectively.

$$R_s = R_0 \cdot exp^{(\beta \cdot T)} \quad (6)$$

In the Van't Hoff model, R_s is the soil respiration rate at a given temperature in ºC (T), R_0 is the soil respiration rate at a reference temperature of 0°C, and β is a fitted slope parameter.

https://doi.org/10.5194/egusphere-2026-4047
Preprint. Discussion started: 20 August 2026

$$R_s = R_0 \cdot exp^{\left[\frac{\beta}{(T+273.15)-d}\right]} \quad (7)$$

For the Lloyd-Taylor model, R_s is the soil respiration rate at a given temperature (T) converted to Kelvin, R_0 is the soil respiration rate when T= the fitted parameter d, and β is an additional fitted slope parameter.

Since we often observed a large increase in soil respiration rates between the 15 and 25 °C incubations followed by apparent saturation, we also tested the performance of a sigmoidal function (Eq. 8), which includes both a temperature inflection point reflecting peak sensitivity as well as saturation after the inflection point (Toms and Lesperance, 2003).

$$R_s = b + \frac{c}{1+\left(\frac{T}{d}\right)^a} \quad (8)$$

In this model, R_s is the soil respiration rate at a given temperature in °C (T), and a, b, c, and d are fitted parameters that adjust the model curve extent in relation to temperature, y-intercept, curve steepness at the inflection point, and where the maximum boundary is first met at the start of the asymptotic phase within the sigmoidal function, respectively.

Model fitting for area-based (F_A) and *SOC*-normalized (F_S) soil respiration was performed using a nonlinear least squares "nls" function in the minpack.lm package (version 1.2.4; Elzhov et al., 2022) in R Core Team (2025). Since the total number of observations varied across decadal warming levels, respiration rates were averaged by level for each incubation step prior to model fitting. This approach was chosen to minimize bias towards levels with more observations, as treatments with larger sample sizes can disproportionately influence the weight of outliers in model fit residuals (Christiansen et al., 2012). Models were first fitted using all data for parameterization, giving globally (i.e. site-level) optimized parameters estimates for each model. Model fitting was then repeated in a step-wise approach using the decadal warming level information, where one, multiple, or all parameters for each model was fit either globally or individually by each decadal warming level. Parameters R_0 and β in the Van't Hoff model, R_0, β, and d in the Lloyd-Taylor model, and b, c, and d in the sigmodal model were adjusted with all data, globally, and by decadal warming level. Parameter a of the sigmoidal function was only adjusted globally, since the model became non-convergent when we attempted to adjust this parameter by decadal warming level. We calculated the coefficient of determination (R^2), root mean square error (RMSE), and Akaike's information corrected criterion (AICc) for each model, and selected the best response function based on whichever had the lowest AICc (Vicca et al., 2014).

Initial F_A calculations were expected to have relatively nominal model uncertainty due to high instrument precision (< 1 ppm CO_2 at 1 Hz) and low detection limitation (0.3, 0.6, and 0.9 ppm CO_2 for 1, 2, and 3 standard deviations, respectively). However, we assumed that *SOC*-based flux normalization would introduce some additional uncertainty by propagated error through supplemental instrumentation when measuring *SOC* concentrations and soil bulk densities. We repeated model fitting for *SOC*-normalized respiration after excluding hotspot (+75 °C) data, where the lowest replication and, therefore, greatest

https://doi.org/10.5194/egusphere-2026-4047
Preprint. Discussion started: 20 August 2026

variability was anticipated. Removing this level allowed us to test whether model selection, specifically the preference for global versus treatment-specific parameterization, was sensitive to elevated uncertainty at the extreme end of our warming gradient. In turn, this helped to further clarify whether the hypothesized decline in area-based soil respiration with increasing decadal warming was principally determined by substrate depletion (model preference for global parameterization in *SOC*-normalized respiration) or other possible underlying mechanisms such as thermal acclimation (model preference for treatment-specific parameterization).

Instead of modeled Q_{10} ($modeled\ Q_{10}$), traditionally calculated using the β parameter from the Van't Hoff model as shown in Eq. (9):

$$modeled\ Q_{10} = exp^{(\beta \cdot 10)} \quad (9)$$

we estimated the modeled *TS* (TS_m) for the best fit Van't Hoff, Lloyd-Taylor and sigmoidal models at each temperature change (5 to 15°C, 15 to 25°C, and 25 to 35°C) for the individual decadal warming level using the optimized parameters selected from these models (Eq. 10):

$$TS_m = \left(\frac{modeled\ R_{s2}}{modeled\ R_{s1}}\right)^{\left(\frac{10}{T_2 - T_1}\right)} \quad (10)$$

where $modeled\ R_{s1}$ and $modeled\ R_{s2}$ are the modeled respiration rates at the lower (T_1) and higher (T_2) incubation temperatures, respectively. Again, since the difference between $T_2 - T_1 = 10$ at the three temperature changes, Eq. 10 can be reduced to $modeled\ R_{s2}$ / $modeled\ R_{s1}$.

3 Results

3.1 SOC, soil bulk density, and vegetation biomass

SOC concentration (%C) declined significantly with increasing decadal warming level (Figure 2A; chi-squared = 173.7, p = 1.2e-35) from a median of 6.30 ± 0.18% (±SE) at ambient decadal warming (+0 °C) to 1.68 ± 0.04% in samples taken from the geothermal hotspot (+75 °C). A substantial reduction was already evident at +1–3 °C with a *SOC* concentration of 4.38 ± 0.21% found at this low decadal warming level. However, there was no clear indication of further loss at either +7–10 °C or +15–20 °C decadal warming with *SOC* concentrations of 4.67 ± 0.08% and 4.84 ± 0.08% at these mid and mid-high levels, respectively. Before soil bulk density correction, *SOC* concentrations appeared to level-off at these low, mid, and mid-high decadal warming levels, with a non-statistically significant difference (Table S1) in concentration of < 0.5% being observed between these groups. This varied substantially from the initial > 1.4% decrease that was seen between the ambient (+0 °C) and low (+1-3 °C) decadal warming levels, as well as the > 1.5% decline in *SOC* concentrations that were observed between

https://doi.org/10.5194/egusphere-2026-4047
Preprint. Discussion started: 20 August 2026

the mid-high (+15-20 °C) and high (+25-35 °C) decadal warming levels. This significant decline resumed again at +25–35 °C decadal warming with an *SOC* concentration of 2.88 ± 0.06% in the high level, continuing to the lowest values observed at +75 °C decadal warming in the hotspot level.

Soil bulk density exhibited a general increasing trend with warming (Figure 2B; chi-squared = 118.3, p = 7.1e-24), rising from a median of 0.70 ± 0.01 g cm^{-3} at ambient (+0 °C) to 0.89 ± 0.02 g cm^{-3} at +1–3 °C decadal warming in the low level. It then dipped at +7–10 °C (0.79 ± 0.01 g cm^{-3}) in the mid decadal warming level, and edged up at +15–20 °C (0.81 ± 0.01 g cm^{-3}) in the mid-high level. Values were highest at the +25–35 °C high decadal warming level (0.97 ± 0.02 g cm^{-3}) and slightly lower at +75 °C decadal warming at the hotspot (0.93 ± 0.01 g cm^{-3}). Pairwise tests (Table S2) indicated the two warmest levels were not different from each other but were higher than cooler treatments, with ambient having the lowest soil bulk density.

After correcting for soil bulk density (Figure 2B), *SOC* stocks in kg C m^{-2} the top soil (3.5 cm), derived from *SOC* concentrations (kg C m^{-3}; Figure S2) and sample depth, also declined significantly (Table S3) with increasing decadal warming level (Figure 2C; chi-squared = 171.9, p = 2.9e-35). Median *SOC* stock decreased from 1.55 ± 0.02 kg C m^{-2} in ambient (+0 °C) decadal warming plots to 0.55 ± 0.02 kg C m^{-2} at the geothermal hotspot (+75 °C). Substantial reductions were evident aside from a slight recovery at the mid-high (+15–20 °C) decadal warming level where stocks were 1.31 ± 0.02 kg C m^{-2}. This was consistent with the brief resurgence at this decadal warming level that was observed in *SOC* concentrations in %C. After correcting for soil bulk density, however, a more gradual decrease in *SOC* stocks occurred between the ambient (+0 °C), the low (+1–3 °C), and mid (+7–10 °C) decadal warming levels compared to *SOC* concentrations in %C. Instead of the more consistent, plateau in *SOC* concentrations (%C) from +1-20 °C decadal warming at the low, mid, and mid-high levels, *SOC* stocks for the low and mid decadal warming levels were 1.47 ± 0.03 kg C m^{-2} and 1.25 ± 0.01 kg C m^{-2}, respectively. *SOC* stocks then declined again quite drastically to 0.92 ± 0.02 kg C m^{-2} for +25–35 °C decadal warming at the high level, ultimately reaching the lowest *SOC* stock of 0.55 ± 0.02 kg C m^{-2} from +75 °C decadal warming at the hotspot.

https://doi.org/10.5194/egusphere-2026-4047
Preprint. Discussion started: 20 August 2026

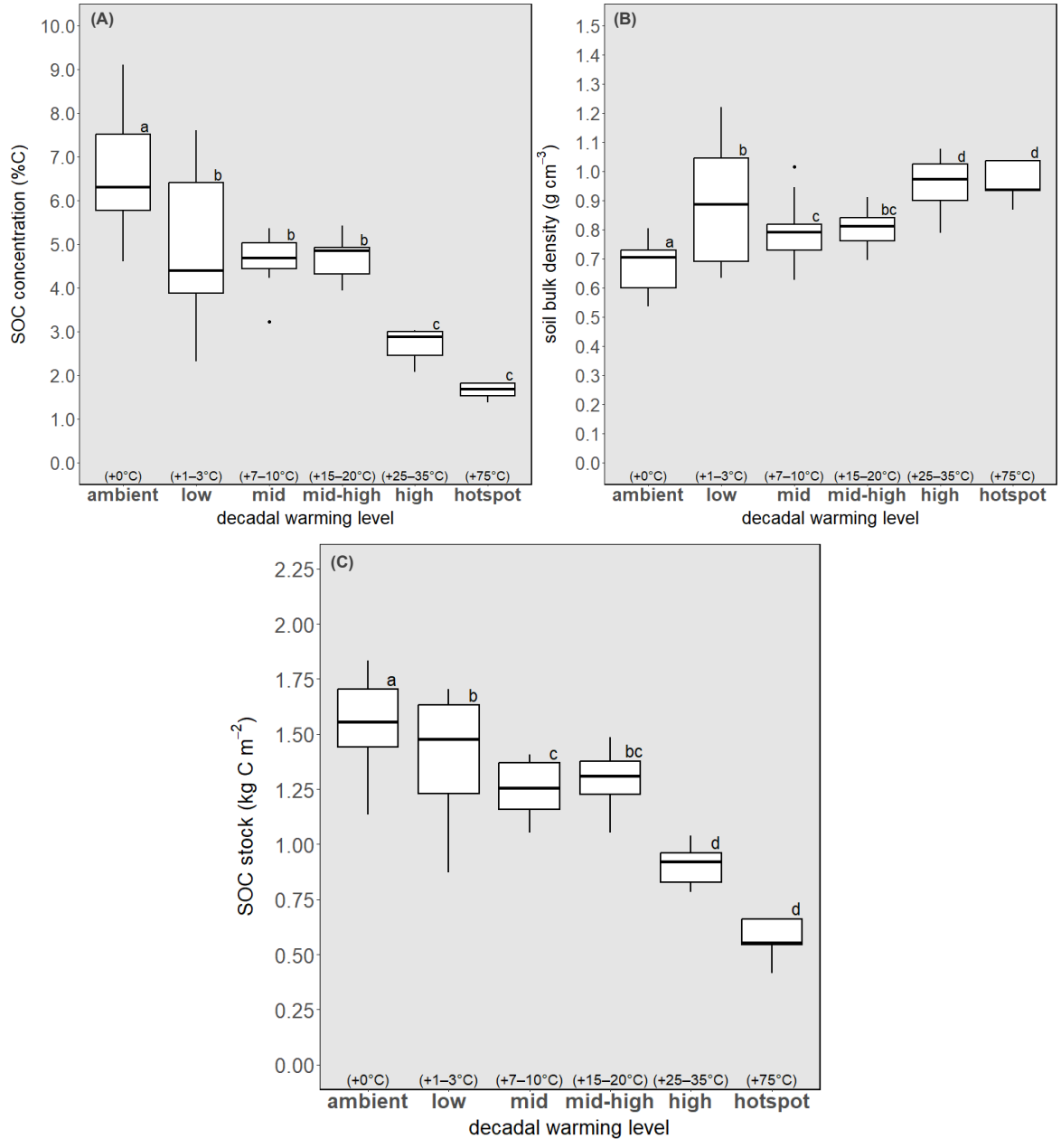

Figure 2. *SOC* concentration in %C (A), dry soil bulk density (ρ_{bulk}) in g cm^{-3} (B), and *SOC* stock in kg C m^{-2} (C) per dried soil core for each decadal warming level. Medians per level indicated by a black line across each box with the interquartile range of point distribution from 25 to 75 percent from the median as box upper and lower limits, and 95% upper and lower standard errors shown as black bars above and below each box. Data outliers that fall outside the bounds of the standard errors are plotted as independent black points. Compact letter display (CLD) in the top right of boxes indicate significant differences ($p \leq 0.05$) between groups.

https://doi.org/10.5194/egusphere-2026-4047
Preprint. Discussion started: 20 August 2026

Vegetation biomass stock (kg m^{-2}) increased significantly with decadal warming up to +15–20 °C, before declining below ambient at the high and hotspot levels (Figure S3; chi-squared = 162.0, p = 3.8e-33). Median total biomass rose from 3.6 ± 0.1 kg m^{-2} in ambient plots to 5.7 ± 0.2 kg m^{-2} at +15–20 °C, while aboveground biomass increased from 3.5 ± 0.2 to 5.5 ± 0.3 kg m^{-2} over the same range. Total and aboveground biomass actually peaked in the +1–3 °C decadal warming level with median stocks of 6.7 ± 0.2 and 6.5 ± 0.2 kg m^{-2}, respectively. At the hotspot, both total and aboveground biomass declined sharply to 1.6 ± 0.1 kg m^{-2}. These values were significantly lower than all other treatments, and were actually the lowest for all decadal warming levels. Post-hoc tests confirmed that vegetation biomass at +15–20 °C was significantly higher than at ambient, low, and hotspot levels, but not distinguishable from +7–10 °C (Table S4). This pattern suggests that moderate warming enhanced plant growth and biomass accumulation, but extreme warming suppressed vegetation productivity, likely due to shifts toward stress-tolerant, low-biomass plant communities. Importantly, the increase in biomass at intermediate warming levels did not translate into higher *SOC* stock, indicating that decomposition processes outpaced OM inputs under prolonged warming.

3.2 Areal and SOC-normalized soil fluxes

On an areal basis, there was a clear decline in the soil CO_2 fluxes with decadal warming from ambient to the +75°C where the model slope and overall flux level decreased with intensity of decadal warming (Figure 3A-3F) following closely to the observed pattern of the decrease in *SOC* stock with intensified decadal warming (Figure 2C).

In the ambient soil there was a mean respiration flux of > 5.5 µmol CO_2 m^{-2} s^{-1} at 35°C, while in the hotspot warming level respiration never exceeded 2 µmol CO_2 m^{-2} s^{-1} at any of the incubation temperatures (Figure 3A-3F). Means of soil respiration per gram soil in µg CO_2–C g $soil^{-1}$ h^{-1} (Figure S8), followed the same response pattern to incubation temperature across decadal warming levels as the CO_2 fluxes on areal basis indicating that the sampled amount of soil in grams per area did not change much across the treatments.

Respiration rates were highest under the warmest incubation condition of 35 °C and lowest at 5°C with the change in rate being the greatest between 15°C and 25°C. Unlike area-based fluxes, soil respiration rates by *SOC* (Figure 3G-3L) were much more similar across the decadal warming levels, with a maximum difference of < 25 µg CO_2–C g SOC^{-1} h^{-1} across levels under the same incubation temperature. However, there was a slight decreasing tendency of rates in the mid-high and high levels before increasing again in the hotspot treatment.

https://doi.org/10.5194/egusphere-2026-4047
Preprint. Discussion started: 20 August 2026

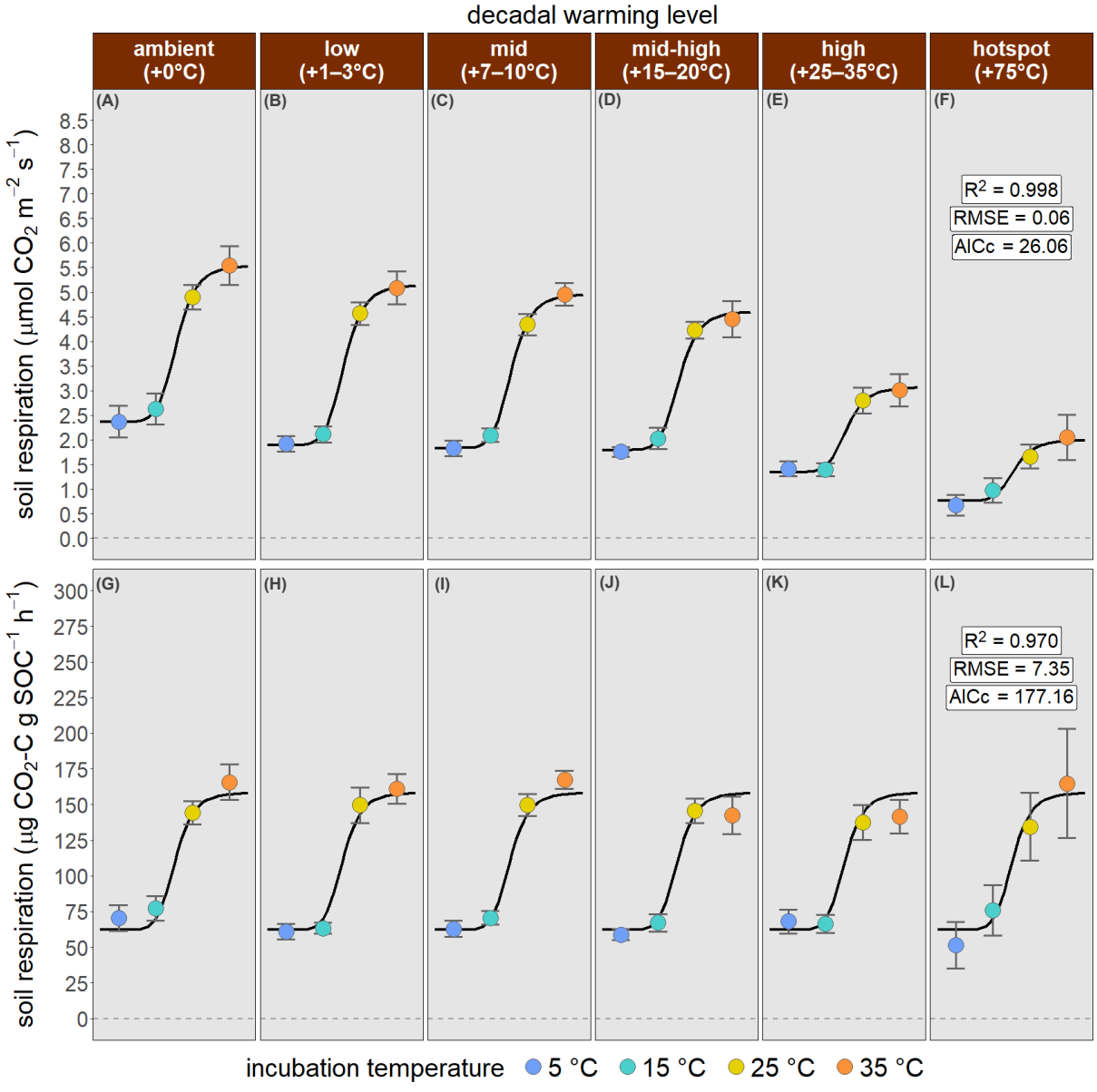

Figure 3. Mean soil respiration rates by area in µmol CO_2 m^{-2} s^{-1} (A-F) and mean soil respiration rates per g *SOC* in µg CO_2-C g SOC^{-1} h^{-1} (G-L) for each incubation temperature (indigo = 5°C, blue = 15°C, lime-green = 25°C, orange = 35°C) with standard error indicated by the black bars. The best fit model for soil respiration by area (sigmoidal model with parameters *b* and *c* fit by decadal warming level and parameters *a* and *d* fit globally) and the best fit model for soil respiration by *SOC* (sigmoidal model with parameters *a*, *b*, *c*, and *d* fit globally) plotted as black lines against the respective (area-based or *SOC*-normalized) mean respiration rates. Values for both models AICc, RMSE, and R^2 are displayed in the upper right-hand corner of F and L panels under the hotspot decadal warming level.

https://doi.org/10.5194/egusphere-2026-4047
Preprint. Discussion started: 20 August 2026

3.3 Modeling temperature responses

Across all 20 area-based soil respiration temperature response models tested in our analysis (Table 1 & Figure S9-28), a sigmoidal model (Figure 3A-3F & Figure S25) showed the best overall fit based on lowest AICc (R^2 = 0.998, RMSE = 0.064, AICc = 26.06). In the best fit model, parameters *b* and *c* were fitted individually by decadal warming level while parameters *a* and *d* were fitted globally. In comparison, the best Van't Hoff and Lloyd-Taylor models had R^2 values ranging 0.918–0.929 (Table 1 & Figure S9-20). For both Van't Hoff and Lloyd-Taylor, the best fit models only allowed R_0 to be fitted by decadal warming level, while remaining parameters for both models were fitted globally. The individual parameter estimates for all tested models on area-based fluxes can be found in Table S9. The best fit sigmoidal model for area-based soil respiration parameters *b* and *c* fitted by decadal warming level showed a distinct pattern with increasing decadal warming (Figure 4). The *b* parameter, which controls the starting point, or y-intercept of the temperature response model, was highest at ambient temperature and declined in a near-linear fashion with decadal warming.

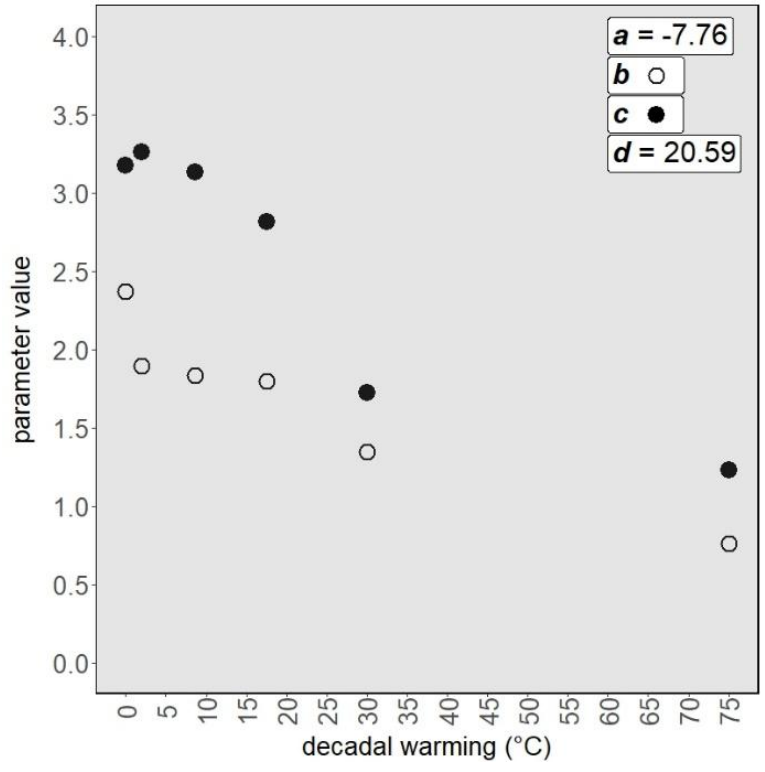

Figure 4. Best fit sigmoidal model for area-based soil respiration with parameters *b* (hollow black dots) and *c* (filled black dots) adjusted by decadal warming level. Parameters *a* and *d* were fit globally (i.e., constants at site-level) with values indicated in the legend (top right).

https://doi.org/10.5194/egusphere-2026-4047
Preprint. Discussion started: 20 August 2026

Still, the values were the closest to each other between the low (+1–3°C), mid (+7–10°C), and mid-high (+15–20°C) decadal warming levels indicating that the baseline, initial respiration between these levels were rather similar and followed the observed pattern of *SOC* changes (Figure 2). The adjusted *c* parameter, which governs the steepness of the sigmoidal rise, peaked at the low decadal warming level (+1–3 °C), was next highest under ambient conditions, and declined across the higher warming levels. This pattern mirrors the *TS* observed for the 15–25 °C incubation interval across the decadal gradient (Figure 5).

Table 1. Model fit statistics for the Van't Hoff, Lloyd-Taylor, and sigmoidal models describing area-based soil respiration (μmol CO_2 m^{-2} s^{-1}) in response to stepwise instantaneous temperature increases. Model type is listed in the "Model" column, while the corresponding fit statistics are presented under the columns labeled "R^2", "RMSE", and "AICc", respectively. In globally (i.e., site-level) parameterized models, parameters were fit to all data, regardless of decadal warming level. These models are labeled "*global*" in the "Parameter Adjusted" column. For decadal warming level (i.e., treatment-level) parameterized models, the parameters listed under this column in italics "*by treatment*" were adjusted individually by decadal warming level. Any parameters not listed "*by treatment*" here were fit globally. For each model type, the best-performing parameterization with the lowest AICc is shown in bold. The best overall model with the lowest AICc across all model types and parameterizations is indicated by asterisks ("**").

Soil Respiration (μmol CO_2 m^{-2} s^{-1}) Model Fit Statistics				
Model	Parameter Adjusted	R^2	RMSE	AICc
Van't Hoff	*global*	0.505	0.996	75.13
Van't Hoff	***R_0 by treatment***	**0.918**	**0.405**	**50.35**
Van't Hoff	*β by treatment*	0.881	0.490	59.47
Van't Hoff	*R_0 & β by treatment*	0.921	0.399	86.46
Lloyd-Taylor	*global*	0.515	0.986	77.53
Lloyd-Taylor	***R_0 by treatment***	**0.929**	**0.376**	**52.07**
Lloyd-Taylor	*β by treatment*	0.927	0.384	53.04
Lloyd-Taylor	*d by treatment*	0.922	0.395	54.35
Lloyd-Taylor	*R_0 & β by treatment*	0.931	0.370	95.00
Lloyd-Taylor	*R_0 & d by treatment*	0.932	0.369	94.97
Lloyd-Taylor	*β & d by treatment*	0.932	0.370	95.00
Lloyd-Taylor	*R_0, β & d by treatment*	0.932	0.368	248.15
Sigmoidal	*global*	0.574	0.924	77.65
Sigmoidal	*b by treatment*	0.939	0.349	54.52
Sigmoidal	*c by treatment*	0.948	0.324	50.92
Sigmoidal	*d by treatment*	0.933	0.368	56.98
Sigmoidal**	***b & c by treatment***	**0.998**	**0.064**	**26.06**
Sigmoidal	*b & d by treatment*	0.972	0.236	88.82
Sigmoidal	*c & d by treatment*	0.954	0.305	101.08
Sigmoidal	*b, c & d by treatment*	0.999	0.048	242.04

https://doi.org/10.5194/egusphere-2026-4047
Preprint. Discussion started: 20 August 2026

Table 2. Model fit statistics for the Van't Hoff, Lloyd-Taylor, and sigmoidal models describing *SOC*-normalized soil respiration (μg CO_2-C g SOC^{-1} h^{-1}) in response to stepwise instantaneous temperature increases. Model type is listed in the "Model" column, while the corresponding fit statistics are presented under the columns labeled "R^2", "RMSE", and "AICc", respectively. In globally (i.e., site-level) parameterized models, parameters were fit to all data, regardless of decadal warming level. These models are labeled "*global*" in the "Parameter Adjusted" column. For decadal warming level (i.e., treatment-level) parameterized models, the parameters listed under this column in italics "*by treatment*" were adjusted individually by decadal warming level. Any parameters not listed "*by treatment*" here were fit globally. Due to model non-convergence, fit statistics for the Lloyd-Taylor model where all parameters were adjusted by decadal warming level ("R_0, β & d *by treatment*") are not reported ("--"). For each model type, the best-performing parameterization with the lowest AICc is shown in bold. The best overall model with the lowest AICc across all model types and parameterizations is indicated by asterisks ("**").

Soil Respiration (μg CO_2-C g SOC^{-1} h^{-1}) Model Fit Statistics				
Model	Parameter Adjusted	R^2	RMSE	AICc
Van't Hoff	***global***	**0.842**	**16.787**	**210.70**
Van't Hoff	*R_0 by treatment*	0.856	16.031	226.89
Van't Hoff	*β by treatment*	0.858	15.896	226.48
Van't Hoff	*R_0 & β by treatment*	0.862	15.667	262.58
Lloyd-Taylor	***global***	**0.863**	**15.633**	**210.19**
Lloyd-Taylor	*R_0 by treatment*	0.876	14.829	228.40
Lloyd-Taylor	*β by treatment*	0.875	14.917	228.69
Lloyd-Taylor	*d by treatment*	0.873	15.014	229.00
Lloyd-Taylor	*R_0 & β by treatment*	0.883	14.423	270.88
Lloyd-Taylor	*R_0 & d by treatment*	0.883	14.416	270.86
Lloyd-Taylor	*β & d by treatment*	0.883	14.424	270.88
Lloyd-Taylor	*R_0, β & d by treatment*	--	--	--
Sigmoidal**	***global***	**0.970**	**7.346**	**177.16**
Sigmoidal	*b by treatment*	0.980	6.011	191.13
Sigmoidal	*c by treatment*	0.974	6.782	196.92
Sigmoidal	*d by treatment*	0.974	6.846	197.37
Sigmoidal	*b & c by treatment*	0.988	4.681	232.20
Sigmoidal	*b & d by treatment*	0.983	5.434	239.36
Sigmoidal	*c & d by treatment*	0.978	6.307	246.51
Sigmoidal	*b, c & d by treatment*	0.992	3.764	451.73

Due to a slight visible decline in *SOC*-normalized respiration being observed with increasing decadal warming, we also tested models on *SOC*-normalized respiration to see if this decline was statistically significant enough for model selection to favor decadal warming level over global (i.e., site-level) parameterization. For *SOC*-normalized soil respiration temperature response models (Table 2 & Figure S29-47), again a sigmoidal model (Figure 3G-L & Figure S40) gave the best fit statistics based on lowest AICc (R^2 = 0.970, RMSE = 7.346, AICc = 177.16). In this model, parameters *a*, *b*, *c*, and *d* were fit globally. For

https://doi.org/10.5194/egusphere-2026-4047
Preprint. Discussion started: 20 August 2026

comparison, the best Van't Hoff and Lloyd-Taylor models had R^2 values ranging from 0.842 – 0.863 (Table 2 & Figure S29-39) and also had all parameters fit globally. The individual optimized model parameters for all tested models on *SOC*-normalized fluxes can be found in Table S10.

3.4 Temperature sensitivity of soil respiration

Since the best fit Van't Hoff model (Table 1) for soil respiration had a globally fitted β parameter, and because the *TS* in the model depends solely on β, TS_m were the same across all decadal warming levels and incubation temperatures (Figure 5A-5C). Similarly, TS_m from the best Lloyd-Taylor model (Table 1) were the same across decadal warming levels and nearly parallel between each temperature incubation change, largely due to intrinsic regulation of *TS* within the Lloyd-Taylor Eq. (Figure 5D-5F).

The best fit sigmoidal model, which was also the best model overall (Table 1), included parameters *b* and *c* fitted individually by each decadal warming level. This made it the only model in which TS_m showed a flexible response to both decadal warming and the three incubation intervals (Figure 5G-5I).

In contrast to the constant (Van't Hoff; Figure 5A-5C) or near-constant (Lloyd-Taylor; Figure 5D-5F) TS_m of the Van't Hoff and Lloyd-Taylor models, TS_o displayed nearly the same kind of dynamic behavior seen in the sigmoidal TS_m, varying systematically among decadal warming level and between incubation interval. For both the 5–15°C (Figure 5A, 5D, & 5G) and 25–35°C (Figure 5C, 5F, & 5I) incubation temperature intervals, TS_o was < 1.5 for all decadal warming levels, with a decreasing trend in TS_o with increasing decadal warming apart from the hotspot. Conversely, the incubation 15–25°C interval (Figure 5B, 5E, & 5H) showed generally higher *TS* as well as an increasing trend with decadal warming level until +15–20°C. After which it only decreased slightly and remained around ~2.

Table 3. Identified rates of soil respiration (μmol CO_2 m^{-2} s^{-1}) at 19.9°C inflection point on the slope of the sigmoidal models with parameters *b* and *c* fitted by decadal warming level and parameters *a* and *d* fitted globally for all data.

Soil Respiration at Sigmoidal Model Inflection Points (19.9°C)	
Decadal Warming Level	Soil Respiration Rate at Inflection (μmol CO_2 m^{-2} s^{-1})
Ambient (+0°C, e.g. no warming)	3.80
Low (+1-3°C above ambient)	3.32
Mid (+7-10°C above ambient)	3.24
Mid-High (+15-20°C above ambient)	2.95
High (+25-35°C above ambient)	2.10
Hotspot (+75°C above ambient)	1.36

https://doi.org/10.5194/egusphere-2026-4047
Preprint. Discussion started: 20 August 2026

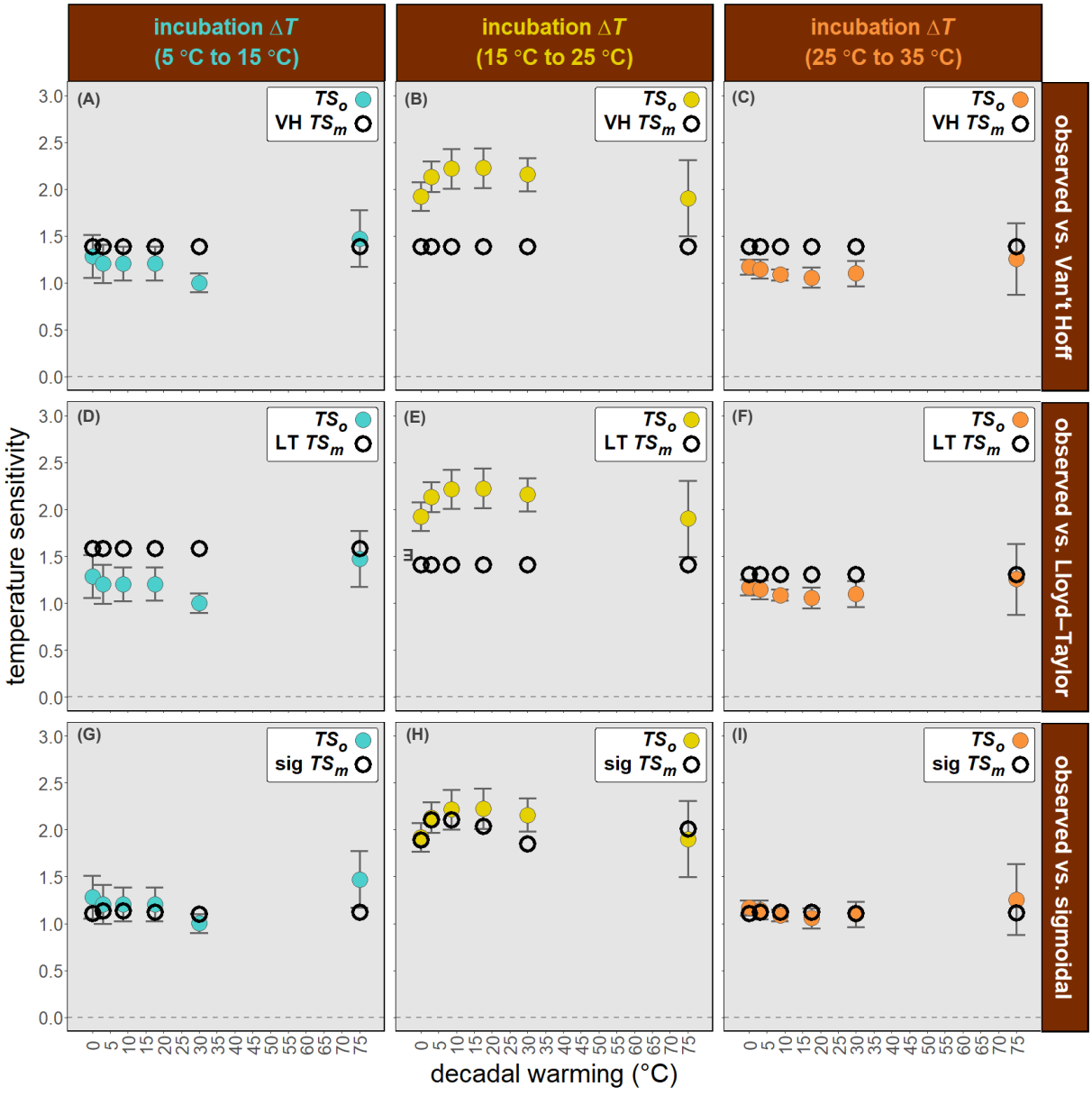

Figure 5. *TS* (unitless) of soil respiration. TS_o explaining observed *TS* between 5-15 °C incubation interval (A, D, & G) indicated as filled blue circles, 15-25 °C incubation interval (B, E, & H) as filled lime-green circles, and 25-35 °C incubation interval (C, F, & I) as filled orange circles with ±SE indicated by the corresponding colored bars. Modeled *TS* (TS_m) for the best fit Van't Hoff (A, B, & C), Lloyd-Taylor (D, E, & F), and sigmoidal (G, H, & I) models shown in black with 5-15 °C incubation interval, 15-25 °C incubation interval, and 25-35 °C incubation interval as hollow circles. Model abbreviations for Van't Hoff (VH), Lloyd-Taylor (LT), and sigmoidal (sig) models shown next to corresponding TS_m in legend. Temperatures on the x-axis are the average temperature above ambient per each decadal warming level.

https://doi.org/10.5194/egusphere-2026-4047
Preprint. Discussion started: 20 August 2026

As a consequence of the near-constant temperature sensitivities of the best fit Van't Hoff and Lloyd-Taylor models for soil respiration, the modeled TS_m differed the most from the observed TS_o for these two models, with especially large discrepancies for the 15–25°C incubation interval (Figure 5). Overall, both models overestimated *TS* for the 5–15°C (Figure 5A & 5D) and 25–35°C (Figure 5C & 5F) incubation intervals, but underestimated *TS* for the 15–25°C interval (Figure 5B & 5E). TS_m from the sigmoidal model (Figure 5G, 5H, & 5I) for soil respiration were generally much closer to the observed TS_o. The sigmoidal model was also able to capture the visible increase in soil respiration response within the 15–25°C incubation interval, i.e. noted by the model inflection point found at 19.9°C (Table 3). The inflection point for the sigmoidal model for soil respiration by *SOC* was in the same location (~20 °C and with a respiration rate of ~110 µg CO_2-C g SOC^{-1} h^{-1}) across decadal warming levels since the best fit model had all parameters fit globally.

4 Discussion

Here we present the first systematic investigation of soil respiration response and *TS* across an extended, decadal-scale warming gradient (+0 to +75 °C) in a subarctic grassland, using intact soil cores to preserve field-relevant conditions. By combining field-derived decadal warming exposure with controlled laboratory incubations across four incremental temperatures, we assessed the *TS* of soil respiration. Through empirical modeling, we showed that compared to traditional models a sigmoidal response function more accurately captured the short-term respiration patterns across a decadal warming gradient, allowing us to identify thermal optima, characterize response thresholds, and reveal that declining respiration with warming was primarily driven by *SOC* depletion, with little indication of soil microbial thermal acclimation.

4.1 SOC depletion under decadal warming

Changes in *SOC* input with soil warming may also play a critical role for *SOC* dynamics (Prommer et al., 2020). Interestingly, the *SOC* concentration (%C) declined in a nonlinear fashion across the decadal warming levels (Figure 2A), with two distinct thresholds of accelerated loss. The first major drop occurred between ambient (+0 °C) and low (+1-3 °C) warming. Concentrations appeared to be consistent between the low (+1-3 °C) to mid-high (+15-20 °C), until a second steep decline followed after +25 °C. For *SOC* stocks in kg m^{-2} (Figure 2C) this decline was more gradual, with a rebound observed between +15-20 °C. This stepwise trajectory suggests that warming can shift soils toward new *SOC* steady states, interrupted by abrupt losses. While previous studies at our site identified a linear relationship between warming and topsoil *SOC* loss up to +6 °C in the first five years of warming (Verbrigghe et al., 2022), our broader decadal warming gradient revealed a more complex, nonlinear pattern of depletion. By extending the thermal gradient beyond temperatures typically deemed most climate relevant, we were able to detect distinct thermal thresholds important for projecting potential *SOC* losses under stronger and/or more prolonged warming. This pattern for *SOC* depletion with more pronounced warming is particularly important, as such conditions are already episodically emerging in high-latitude ecosystems.

https://doi.org/10.5194/egusphere-2026-4047
Preprint. Discussion started: 20 August 2026

Despite observed increases in plant biomass production and extended growing seasons under warming at this site (Leblans et al., 2017; Mortier et al., 2024) *SOC* stocks have not increased (Figure 2C) at decadal warming levels where vegetation growth was actually higher than ambient. We did see a rise in vegetation biomass stock with warming up to +20 °C (Figure S3; Table S4) reflecting likely augmented organic matter (OM) deposition into these soils within these warming conditions. While vegetation stocks indicate increased plant growth rates with increased decadal warming of up to 15-20 °C above ambient, the likely increase in OM deposition from increased litter input to the soil was not reflected in the total *SOC* content. These discrepancies suggest that accelerated decomposition quite possibly outpaced heightened OM inputs within this warming range (Meeran et al., 2023). The rise in fresh plant inputs may have also induced positive priming of native *SOC*, which tends to intensify under warming (Crowther et al., 2016; Tao et al., 2024), resulting in net *SOC* losses despite greater primary productivity relative to ambient.

Besides biological feedbacks, mineral factors may also influence *SOC* loss. Higher soil bulk density (Figure 2B) points to a minor compaction effect (Fleming et al., 2006) explaining the more gradual *SOC* stock depletion with warming compared to *SOC* concentration (%C) after correcting for differences in soil bulk density. This shift toward a more mineral-rich and carbon-poor matrix is consistent with steady declines in %C (Figure 2C). The slight increase in soil bulk density with warming may reflect soil compaction, OM loss, or reduced root biomass, which in turn could explain the relatively elevated *SOC* observed in the +15–20 °C range despite overall declining trends. This behavior likely reflects Andosol traits whereby high microporosity and strong mineral–organic ass*oc*iations enhance surface area sorption, allowing soils to retain higher *SOC* fractions and buffer losses at intermediate warming (Calabi-Floody et al., 2015; Chevallier et al., 2010; Matus et al., 2014; Shimada et al., 2022). More carbon may now be processed through biomass and respiration, but less could be retained in the soil once an upper limit on mineral-ass*oc*iated *SOC* is reached (Matus et al., 2024; Sadatshojaei et al., 2021; Wang et al., 2021). Such a limit could help to explain why larger plant inputs (Figure S3; Table S4) do not necessarily translate to increased *SOC* storage (Figure 2A).

4.2 Respiration responses and underlying controls

To contextualize the magnitude of measured respiration rates in this study, we compared both *SOC*-normalized and area-based values at 15 °C to those reported for high-latitude soils within similar conditions. *SOC*-normalized respiration rates across warming levels ranged from approximately 65 to 105 μg CO_2–C g^{-1} *SOC* h^{-1} (Figure 3G-3L), aligning well with previously reported values for subarctic and boreal soils, which typically span 50–150 (200) μg C g^{-1} *SOC* h^{-1} at comparable temperatures (Karhu et al., 2014; Karhu et al., 2010; Hartley et al., 2007; Hartley et al., 2008; Ťupek et al., 2024; Wang et al., 2021; Bradley-Cook et al., 2016). Likewise, area-based respiration rates ranged from ~1.6 to 3.8 μmol CO_2 m^{-2} s^{-1} across warming levels (Figure 3A-3F), consistent with published values for high-latitude soils, generally falling within the range of ~1.3–6.0 μmol CO_2 m^{-2} s^{-1} at 10–15 °C (Protti-Sánchez et al., 2025; Smith and Johnson, 2004; Ge et al., 2017; Cahoon et al., 2016; Maljanen et al., 2019; André and Bondesson, 2014). This concordance supports the reliability of our incubation approach and

https://doi.org/10.5194/egusphere-2026-4047
Preprint. Discussion started: 20 August 2026

indicates that the observed respiration patterns are not the result of anomalously high or low baseline activity. Rather, they reflect genuine shifts associated with warming exposure.

We observed that soil respiration rates (Figure 3A-3F) declined markedly with increasing decadal warming**,** particularly for area-based fluxes**.** Ambient and low warming treatments exhibited the highest respiration, which then progressively diminished with further temperature exposure, pointing to reduced activity under sustained warming. However, normalizing respiration by *SOC* (Figure 3G-3L) largely eliminated this decline with increasing decadal warming level. Based off of this continuity in *SOC*-normalized respiration we can infer that reductions in area-based respiration were driven primarily by substrate availability rather than by thermal acclimation. Our findings align with results from other long-term warming experiments which similarly observed stable microbial respiration per gram of *SOC* and found that microbes maintained their respiratory capacity per unit *SOC* at warming levels of up to +6 °C. They concluded that substrate depletion, not downregulation, as the dominant control for respiration loss (Walker et al., 2018; Hartley et al., 2007; Hartley et al., 2008; Radujković et al., 2018).

Under warming and substrate-limited conditions, soil microbes appear to alter their carbon allocation strategies, potentially reflecting a decline in carbon use efficiency (CUE). Microbial CUE may diminish such that a greater proportion of assimilated carbon is respired for maintenance instead of redirected to biomass production (Walker et al., 2018; Tucker et al., 2013; Zhang et al., 2024; Liang et al., 2024) reinforcing the central role of microbial metabolism in *SOC* accrual. Their high affinity for stabilizing *SOC* coupled with a further reduction in bioavailability with warming exposes a considerable limitation on soil respiration. However, this stabilization potential may be limited by nutrient constraints, such as nitrogen (Figure S4-S5; Table S5-S6), which reduce microbial efficiency and amplify mismatches between carbon inputs and losses (Meeran et al., 2023).

4.3 Modeling respiration responses and implications for SOC dynamics

Commonly used models, such as Van't Hoff and Lloyd-Taylor, thus far have struggled to capture the behavior of change in respiration rates with direct warming where first temperature response is low, then it increase at a greater rate until they reach a point where they drop off again (Alster et al., 2023). This was also the case in our study where the sigmoidal function proved to be the most reliable in capturing the best fit across our full temperature range, i.e. yielding low activity at cooler temperatures, rapid increases between ~15–25 °C, and saturation on the highest end for both respiration by area (Figure 3A-3F; Table 1) and normalized by *SOC* (Figure 3G-3L; Table 2). The best fit model for area-based fluxes indicated apparent changes in *TS* through the decreasing trend we observed in parameters *b* and *c* (Figure 4). Furthermore, when respiration rates were normalized by *SOC* the best fit models selected for global (i.e., site-level) parameterization (Table 2). With this selection, *SOC*-normalized respiration appeared relatively consistent across the decadal warming gradient supporting the interpretation that reductions in areal respiration were driven primarily by declining substrate availability rather than microbial thermal acclimation. This has major implications for projecting future *SOC* under warming because we can more accurately model the

https://doi.org/10.5194/egusphere-2026-4047
Preprint. Discussion started: 20 August 2026

observed behavior of soil reparation to better reflect these processes in our predictive estimates of *SOC* turnover (Wieder et al., 2013; Berardi et al., 2024; Schwarz et al., 2024).

4.4 Temperature sensitivity across warming gradients and timescales

A key finding from our incubations was that TS_o differed across decadal warming levels and incubation temperature intervals in distinct, context-dependent ways (Figure 5), reflecting the combined effects of immediate temperature and prolonged warming exposure on microbial activity (Weedon et al., 2023; Bastida et al., 2019). This variable behavior underscores the combined effects of differing warming intensity and exposure time, emphasizing the profound influence both have on *SOC* turnover. Respiration responses were more temperature sensitive at lower decadal warming levels, while at increasing levels of warming the response was dampened, likely reflecting microbial communities adapted to substrate-limited environments where resources are preferentially allocated to maintenance over growth or productivity (Tucker et al., 2013; Karhu et al., 2014; Li et al., 2023; Čapek et al., 2019; Crowther and Bradford, 2013). This is consistent with previous research showing diminished responsiveness under low-temperature conditions following prolonged warming (Sampath et al., 2023; Du et al., 2023). Thus, soils exposed to less warming remain more responsive to low temperature changes, while those that have undergone extended warming appear more fundamentally constrained.

TS across all decadal warming treatments peaked between incubation temperatures of 15–25 °C. Although peak magnitude varied relative to long-term warming intensity, peak position within this instantaneous thermal window was conserved (e.g., the highest TS_o occurred at +7–10 °C decadal warming within this 15–25 °C incubation interval). The heightened *TS* observed within this 15–25 °C interval points to a thermal optimum for microbial activity, where fundamental shifts in physiology and/or community composition (Zhang et al., 2024) may maximize respiration under favorable but sub-saturating thermal conditions (Alster et al., 2023). Such responses may reflect microbial adaptation via physiological changes**,** such as altered enzyme allocation or ribosomal downregulation under warming (Söllinger et al., 2024). These patterns indicate that prolonged warming altered the magnitude of the response but not the temperature at which maximum sensitivity occurred. This is consistent with a shared thermal optimum and a narrowing functional range for respiration that remained stable despite differences in decadal warming extent. Notably, this elevated sensitivity appeared thermally bounded, with temperature sensitivities decreasing at both lower (5–15 °C) and higher (25–35 °C) incubation intervals. The differential responses across these intervals indicate that the reduction in respiration under extended warming is not a uniform suppression. Rather, it likely reflects emergent shifts in ecosystem structure, physiological regulation, and carbon-use strategies driven by thermal conditions and changing substrate composition. An apparent restriction of the effective temperature window, coupled with accelerated decomposition within it, suggests that brief episodes of vigorous activity ("hot moments") may play an increasingly influential role in annual *SOC* turnover. This is particularly relevant for periods of profound warming where soils are pushed into this window of amplified biological responsiveness. TS_o remained the most stable across decadal warming levels in the 25–35 °C interval suggesting that respiration also approaches a saturation point at higher temperatures, supported by known thermal limits to cellular

https://doi.org/10.5194/egusphere-2026-4047
Preprint. Discussion started: 20 August 2026

function (Wang et al., 2021; Liu et al., 2018; Knapp and Huang, 2022). Together, these results imply that *SOC* turnover is likely to be most responsive under mid-range decadal warming conditions when *in situ* soil temperatures fall within this 15–25 °C thermal optimum.

5 Conclusions

Limitations to our study include soil sampling limited to one time point (early autumn) rather than seasonally comprehensive sampling, a focus on the topsoil horizon (i.e., upper 5 cm), slightly unbalanced replication between decadal warming levels (i.e., fewer plots at the warmest end of the geothermal gradient), and absence of microbial or substrate-level measurements to mechanistically disentangle microbial thermal acclimation from changes in carbon quality. Nonetheless, our incubation of intact cores across a natural geothermal gradient showed how decades of warming alter *SOC* dynamics and *TS* in a subarctic grassland.

SOC losses increased with decadal warming but followed a nonlinear pattern with abrupt thresholds at +10 °C and + 20 °C warming, respectively, where *SOC* losses decreased dramatically. *SOC*-normalized respiration was relatively constant across decadal warming treatments, suggesting that substrate depletion rather than physiological downregulation is primarily responsible for the area-based respiration decline. This was further supported by all decadal warming levels showing the highest *TS* within the same instantaneous 15–25 °C interval. In conclusion, across the broad decadal warming range in our study no evidence of thermal microbial acclimation was found, suggesting that other factors (e.g. direct climate variables, plant community composition and activity, etc.) drive *SOC* loss in response to warming.

The consistently higher *TS* in the 15–25 °C interval, was well-captured only by a sigmoidal response function stressing the fundamental limitation of applying models with fixed *TS* (e.g., Q_{10}) to upscale or predict *SOC* loss potential. Reliable projections of *SOC* turnover will require adaptive, process-based models that allow *TS* to change dynamically with temperature and are able to reproduce non-linear, stepwise development of *SOC* stocks with warming. This imperative is especially true in high-latitude systems, where rapid and persistent warming is progressively amplifying both vulnerability and uncertainty over time.

Code and data availability

The data and core R code supporting the findings of this study are currently being prepared for public release and are intended to be deposited in the DeiC Dataverse repository, where they will be assigned DOIs once preparation is complete. Preparation includes documentation, organization, and archiving of the datasets and analysis code to facilitate their use by readers and enable reproducibility of the results. Public access to the data and code, together with the associated repository records and

https://doi.org/10.5194/egusphere-2026-4047
Preprint. Discussion started: 20 August 2026

DOIs, will be provided prior to final publication of this manuscript. Until then, the data and code are available from the corresponding authors upon reasonable request.

Supplement link

The link to the supplement to be included by Copernicus

Author contributions

LMA, JRC, BDS, and KSL conceived the study and developed the methodology. LMA and KSL curated the data, performed the formal analyses, and developed the software. LMA, JRC, BDS, and KSL carried out the investigation and provided resources. BDS and KSL secured funding and supervised the project, and LMA, BDS, and KSL oversaw project administration. LMA, JRC, BDS, and KSL validated the results. LMA and KSL prepared the visualizations. LMA wrote the manuscript with contributions from JRC, BDS, and KSL.

Competing interests

The authors declare that they have no conflicts of interest in Copernicus Publications as an integral part of transparent recording of scientific work.

Disclaimer

Copernicus Publications remains neutral with regard to jurisdictional claims made in the text, published maps, institutional affiliations, or any other geographical representation in this paper. While Copernicus Publications makes every effort to include appropriate place names, the final responsibility lies with the authors. Views expressed in the text are those of the authors and do not necessarily reflect the views of the publisher.

Acknowledgements

This research was financially supported by the FutureArctic project, a European Union's Horizon 2020 framework program for research and innovation under the Marie Skłodowska-Curie Actions (Grant No. 813114). Automatic chambers were kindly provided by AnaEE Denmark (anaee.dk).

https://doi.org/10.5194/egusphere-2026-4047
Preprint. Discussion started: 20 August 2026

Financial support

Support funds from the FutureArctic project, a European Union's Horizon 2020 framework program for research and innovation under the Marie Skłodowska-Curie Actions. Grant agreement number for this project is 813114.

Review statement

The review statement to be added by Copernicus Publications listing the handling editor as well as all contributing referees according to their status anonymous or identified

References

Alster, C. J., van de Laar, A., Goodrich, J. P., Arcus, V. L., Deslippe, J. R., Marshall, A. J., and Schipper, L. A.: Quantifying thermal adaptation of soil microbial respiration, Nature Communications, 14, 5459, 10.1038/s41467-023-41096-x, 2023.

André, H. and Bondesson, A.: Hur en ökad marktemperatur påverkar fotosyntes och markrespiration i en boreal skog, Swedish University of Agricultural Sciences (SLU), Dept. of Soil and Environment, Uppsala, Sweden, 2014.

Arnalds, Ó.: The Soils of Iceland, Springer, Dordrecht, Heidelberg, New York, London2015.

Azizi-Rad, M., Guggenberger, G., Ma, Y., and Sierra, C. A.: Sensitivity of soil respiration rate with respect to temperature, moisture and oxygen under freezing and thawing, Soil Biology and Biochemistry, 165, 108488, https://doi.org/10.1016/j.soilbio.2021.108488, 2022.

Bastida, F., García, C., Fierer, N., Eldridge, D. J., Bowker, M. A., Abades, S., Alfaro, F. D., Asefaw Berhe, A., Cutler, N. A., Gallardo, A., García-Velázquez, L., Hart, S. C., Hayes, P. E., Hernández, T., Hseu, Z.-Y., Jehmlich, N., Kirchmair, M., Lambers, H., Neuhauser, S., Peña-Ramírez, V. M., Pérez, C. A., Reed, S. C., Santos, F., Siebe, C., Sullivan, B. W., Trivedi, P., Vera, A., Williams, M. A., Luis Moreno, J., and Delgado-Baquerizo, M.: Global ecological predictors of the soil priming effect, Nature Communications, 10, 3481, 10.1038/s41467-019-11472-7, 2019.

Berardi, D. M., Hartman, M. D., Brzostek, E. R., Bernacchi, C. J., DeLucia, E. H., von Haden, A. C., Kantola, I., Moore, C. E., Yang, W. H., Hudiburg, T. W., and Parton, W. J.: Microbial-explicit processes and refined perennial plant traits improve modeled ecosystem carbon dynamics, Geoderma, 443, 116851, https://doi.org/10.1016/j.geoderma.2024.116851, 2024.

Bond-Lamberty, B., Bailey, V. L., Chen, M., Gough, C. M., and Vargas, R.: Globally rising soil heterotrophic respiration over recent decades, Nature, 560, 80-83, 2018.

Boyd, R. J., Powney, G. D., Burns, F., Danet, A., Duchenne, F., Grainger, M. J., Jarvis, S. G., Martin, G., Nilsen, E. B., and Porcher, E.: ROBITT: A tool for assessing the risk-of-bias in studies of temporal trends in ecology, Methods in Ecology and Evolution, 13, 1497-1507, 2022.

https://doi.org/10.5194/egusphere-2026-4047
Preprint. Discussion started: 20 August 2026

Bradley-Cook, J. I., Petrenko, C. L., Friedland, A. J., and Virginia, R. A.: Temperature sensitivity of mineral soil carbon decomposition in shrub and graminoid tundra, west Greenland, Climate Change Responses, 3, 2, 10.1186/s40665-016-0016-1, 2016.

Cahoon, S. M. P., Sullivan, P. F., Gamm, C., Welker, J. M., Eissenstat, D., and Post, E.: Limited variation in proportional contributions of auto- and heterotrophic soil respiration, despite large differences in vegetation structure and function in the Low Arctic, Biogeochemistry, 127, 339-351, 2016.

Calabi-Floody, M., Rumpel, C., Velásquez, G., Violante, A., Bol, R., Condron, L. M., and Mora, M. L.: Role of Nanoclays in Carbon stabilization in Andisols and Cambisols, Journal of soil science and plant nutrition, 15, 587-604, 2015.

Čapek, P., Starke, R., Hofmockel, K. S., Bond-Lamberty, B., and Hess, N.: Apparent temperature sensitivity of soil respiration can result from temperature driven changes in microbial biomass, Soil Biology and Biochemistry, 135, 286-293, https://doi.org/10.1016/j.soilbio.2019.05.016, 2019.

Chevallier, T., Woignier, T., Toucet, J., and Blanchart, E.: Organic carbon stabilization in the fractal pore structure of Andosols, Geoderma, 159, 182-188, https://doi.org/10.1016/j.geoderma.2010.07.010, 2010.

Christiansen, J. R., Vesterdal, L., and Gundersen, P.: Nitrous oxide and methane exchange in two small temperate forest catchments—effects of hydrological gradients and implications for global warming potentials of forest soils, Biogeochemistry, 107, 437-454, 10.1007/s10533-010-9563-x, 2012.

Crowther, T., Todd-Brown, K., Rowe, C., Wieder, W., Carey, J., Machmuller, M., Snoek, B., Fang, S., Zhou, G., Allison, S., Blair, J., Bridgham, S., Burton, A., Carrillo, Y., Reich, P., Clark, J., Classen, A., Dijkstra, F., Elberling, B., and Bradford, M.: Quantifying global soil carbon losses in response to warming, Nature, 540, 104-108, 10.1038/nature20150, 2016.

Crowther, T. W. and Bradford, M. A.: Thermal acclimation in widespread heterotrophic soil microbes, Ecology Letters, 16, 469-477, https://doi.org/10.1111/ele.12069, 2013.

Cruz-Paredes, C., Tájmel, D., and Rousk, J.: Variation in Temperature Dependences across Europe Reveals the Climate Sensitivity of Soil Microbial Decomposers, Applied and Environmental Microbiology, 89, e02090-02022, 10.1128/aem.02090-22, 2023.

Du, Y., Mohan, J. E., Frankson, P., and Sihi, D.: Decoding the Hidden Mechanisms of Soil Carbon Cycle in Response to Climate Change, AGU Fall Meeting Abstracts, San Francisco, CA, December 01, 20232023.

Elzhov, T. V., Mullen, K. M., Spiess, A., and Bolker, B.: minpack.lm: R Interface to the Levenberg-Marquardt Nonlinear Least-Squares Algorithm Found in MINPACK, Plus Support for Bounds (R package version 1.2-2) [code], 2022.

Fang, C. and Moncrieff, J.: The dependence of soil CO2 efflux on temperature, Soil Biology and Biochemistry, 33, 155-165, 2001.

Food and Agriculture Organization (FAO) of the United Nations: Soil Sampling and Analysis: Technical Guidelines, Rome, Italy, FAO Soils Bulletin, 105, https://doi.org/10.4060/ca2796en, 2020.

Fleming, R. L., Powers, R. F., Foster, N. W., Kranabetter, J. M., Scott, D. A., Ponder, F., Jr., Berch, S., Chapman, W. K., Kabzems, R. D., Ludovici, K. H., Morris, D. M., Page-Dumroese, D. S., Sanborn, P. T., Sanchez, F. G., Stone, D. M., and

https://doi.org/10.5194/egusphere-2026-4047
Preprint. Discussion started: 20 August 2026

Tiarks, A. E.: Effects of organic matter removal, soil compaction, and vegetation control on 5-year seedling performance: a regional comparison of Long-Term Soil Productivity sites, Canadian Journal of Forest Research, 36, 529-550, 10.1139/x05-271, 2006.

Foereid, B., Ward, D. S., Mahowald, N., Paterson, E., and Lehmann, J.: The sensitivity of carbon turnover in the Community Land Model to modified assumptions about soil processes, EARTH SYSTEM DYNAMICS, 5, 211-221, 10.5194/esd-5-211-2014, 2014.

Franzson, H., G.H, G., Helgadóttir, H., and Frolova, J.: Porosity, density and chemical composition relationships in altered Icelandic hyaloclastites, 2010.

Ge, L., Lafleur, P. M., and Humphreys, E. R.: Respiration from Soil and Ground Cover Vegetation Under Tundra Shrubs, Arctic, Antarctic, and Alpine Research, 49, 537-550, 10.1657/AAAR0016-064, 2017.

Halldórsson, B. and Sigbjörnsson, R.: The Mw6.3 Ölfus earthquake at 15:45 UTC on 29 May 2008 in South Iceland: ICEARRAY strong-motion recordings, Soil Dynamics and Earthquake Engineering, 29, 1073-1083, https://doi.org/10.1016/j.soildyn.2008.12.006, 2009.

Hartley, I. P., Heinemeyer, A., and Ineson, P.: Effects of three years of soil warming and shading on the rate of soil respiration: substrate availability and not thermal acclimation mediates observed response, Global Change Biology, 13, 1761-1770, https://doi.org/10.1111/j.1365-2486.2007.01373.x, 2007.

Hartley, I. P., Hopkins, D. W., Garnett, M. H., Sommerkorn, M., and Wookey, P. A.: Soil microbial respiration in arctic soil does not acclimate to temperature, Ecology Letters, 11, 1092-1100, https://doi.org/10.1111/j.1461-0248.2008.01223.x, 2008.

Icelandic Meteorological Office (IMO): Climate archives for weather stations, http://www.vedur.is/vedur/vedurfar/medaltalstoflur/, last access: 23 July 2024.

Intergovernmental Panel on Climate Change (IPCC): The Ocean and Cryosphere in a Changing Climate: Special Report of the Intergovernmental Panel on Climate Change, Cambridge, 9781009157964, 203-320, DOI: 10.1017/9781009157964.005, 2022.

Intergovernmental Panel on Climate, Change (IPCC): Climate Change 2022 – Impacts, Adaptation and Vulnerability: Working Group II Contribution to the Sixth Assessment Report of the Intergovernmental Panel on Climate Change, Cambridge, 9781009325837, 2319-2368, DOI: 10.1017/9781009325844.023, 2023.

Ito, A., Nishina, K., and Noda, H. M.: Impacts of future climate change on the carbon budget of northern high-latitude terrestrial ecosystems: An analysis using ISI-MIP data, Polar Science, 10, 346-355, https://doi.org/10.1016/j.polar.2015.11.002, 2016.

Jian, J., Bond-Lamberty, B., Hao, D., Sulman, B. N., Patel, K. F., Zheng, J., Dorheim, K., Pennington, S. C., Hartman, M. D., and Warner, D.: Leveraging observed soil heterotrophic respiration fluxes as a novel constraint on global-scale models, Global Change Biology, 27, 5392-5403, 2021.

Johannesson, B.: The Soils of Iceland. University Research Institute, Reykjavik, Iceland, Agricultural Research Institute, 1960.

https://doi.org/10.5194/egusphere-2026-4047
Preprint. Discussion started: 20 August 2026

Kan, Z.-R., Liu, W.-X., Liu, W.-S., He, C., Bohoussou, N. d. Y., Dang, Y. P., Zhao, X., and Zhang, H.-L.: Sieving soil before incubation experiments overestimates carbon mineralization but underestimates temperature sensitivity, Science of The Total Environment, 806, 150962, https://doi.org/10.1016/j.scitotenv.2021.150962, 2022.

Karhu, K., Fritze, H., Tuomi, M., Vanhala, P., Spetz, P., Kitunen, V., and Liski, J.: Temperature sensitivity of organic matter decomposition in two boreal forest soil profiles, Soil Biology and Biochemistry, 42, 72-82, https://doi.org/10.1016/j.soilbio.2009.10.002, 2010.

Karhu, K., Auffret, M. D., Dungait, J. A. J., Hopkins, D. W., Prosser, J. I., Singh, B. K., Subke, J.-A., Wookey, P. A., Ågren, G. I., Sebastià, M.-T., Gouriveau, F., Bergkvist, G., Meir, P., Nottingham, A. T., Salinas, N., and Hartley, I. P.: Temperature sensitivity of soil respiration rates enhanced by microbial community response, Nature, 513, 81-84, 10.1038/nature13604, 2014.

Knapp, B. D. and Huang, K. C.: The Effects of Temperature on Cellular Physiology, Annual Review of Biophysics, 51, 499-526, https://doi.org/10.1146/annurev-biophys-112221-074832, 2022.

Kristinsson, H.: A Guide to the Flowering Plants of Iceland, 10.2307/25065459, 2010.

Leblans, N. I. W., Sigurdsson, B. D., Vicca, S., Fu, Y., Penuelas, J., and Janssens, I. A.: Phenological responses of Icelandic subarctic grasslands to short-term and long-term natural soil warming, Global Change Biology, 23, 4932-4945, https://doi.org/10.1111/gcb.13749, 2017.

Li, J., Pei, J., Fang, C., Li, B., and Nie, M.: Thermal adaptation of microbial respiration persists throughout long-term soil carbon decomposition, Ecology Letters, 26, 1803-1814, https://doi.org/10.1111/ele.14296, 2023.

Li, Q., Guo, J., Wang, Z., Wang, C., Liu, P., Lv, G., Yang, Z., Wang, C., and Qiu, X.: Effects of Warming and Increased Precipitation on Root Production and Turnover of Stipa breviflora Community in Desert Steppe, Agronomy, 14, 1521, https://doi.org/10.3390/agronomy14071521, 2024.

Liang, Z., Guo, X., Liu, S., Su, Y., Zeng, Y., Xie, C., Gao, Q., Lei, J., Li, B., Wang, M., Dai, T., Ma, L., Fan, F., Yang, Y., Liu, X., and Zhou, J.: Microbial mediation of soil carbon loss at the potential climax of alpine grassland under warming, Soil Biology and Biochemistry, 192, 109395, https://doi.org/10.1016/j.soilbio.2024.109395, 2024.

Liu, Y., He, N., Wen, X., Xu, L., Sun, X., Yu, G., Liang, L., and Schipper, L. A.: The optimum temperature of soil microbial respiration: Patterns and controls, Soil Biology and Biochemistry, 121, 35-42, https://doi.org/10.1016/j.soilbio.2018.02.019, 2018.

Lloyd, J. and Taylor, J. A.: On the Temperature Dependence of Soil Respiration, Functional Ecology, 8, 315-323, 10.2307/2389824, 1994.

Loock, S. V.: Short-trem and long-term changes in vegetation and biomass in response to natural soil warming and nitrogen availability in a subarctic grassland., Faculty of Science, Department of Biology, Unviersity of Antwerp, 49 pp., 2017.

Maes, S. L., Dietrich, J., Midolo, G., Schwieger, S., Kummu, M., Vandvik, V., Aerts, R., Althuizen, I. H. J., Biasi, C., Björk, R. G., Böhner, H., Carbognani, M., Chiari, G., Christiansen, C. T., Clemmensen, K. E., Cooper, E. J., Cornelissen, J. H. C., Elberling, B., Faubert, P., Fetcher, N., Forte, T. G. W., Gaudard, J., Gavazov, K., Guan, Z., Guðmundsson, J., Gya,

https://doi.org/10.5194/egusphere-2026-4047
Preprint. Discussion started: 20 August 2026

R., Hallin, S., Hansen, B. B., Haugum, S. V., He, J. S., Hicks Pries, C., Hovenden, M. J., Jalava, M., Jónsdóttir, I. S., Juhanson, J., Jung, J. Y., Kaarlejärvi, E., Kwon, M. J., Lamprecht, R. E., Le Moullec, M., Lee, H., Marushchak, M. E., Michelsen, A., Munir, T. M., Myrsky, E. M., Nielsen, C. S., Nyberg, M., Olofsson, J., Óskarsson, H., Parker, T. C., Pedersen, E. P., Petit Bon, M., Petraglia, A., Raundrup, K., Ravn, N. M. R., Rinnan, R., Rodenhizer, H., Ryde, I., Schmidt, N. M., Schuur, E. A. G., Sjögersten, S., Stark, S., Strack, M., Tang, J., Tolvanen, A., Töpper, J. P., Väisänen, M. K., van Logtestijn, R. S. P., Voigt, C., Walz, J., Weedon, J. T., Yang, Y., Ylänne, H., Björkman, M. P., Sarneel, J. M., and Dorrepaal, E.: Environmental drivers of increased ecosystem respiration in a warming tundra, Nature, 629, 105-113, 10.1038/s41586-024-07274-7, 2024.

Maier, M., Weber, T. K., Fiedler, J., Fuss, R., Glatzel, S., Huth, V., Jordan, S., Jurasinski, G., Kutzbach, L., and Schäfer, K.: Introduction of a guideline for measurements of greenhouse gas fluxes from soils using non-steady-state chambers, Journal of Plant Nutrition and Soil Science, 185, 447-461, 2022.

Maljanen, M., Yli-Moijala, H., Sigurdsson, B. D., and Biasi, C.: Abiotic CO2 sources confound interpretation of temperature responses of in situ respiration in geothermally warmed forest soils of Iceland, Biogeosciences Discuss., 2019, 1-22, 10.5194/bg-2019-213, 2019.

Matus, F., Rumpel, C., Neculman, R., Panichini, M., and Mora, M. L.: Soil carbon storage and stabilisation in andic soils: A review, CATENA, 120, 102-110, https://doi.org/10.1016/j.catena.2014.04.008, 2014.

Matus, F. J., Paz-Pellat, F., Covaleda, S., Etchevers, J. D., Hidalgo, C., and Báez, A.: Upper limit of mineral-associated organic carbon in temperate and sub-tropical soils: How far is it?, Geoderma Regional, 37, e00811, https://doi.org/10.1016/j.geodrs.2024.e00811, 2024.

Mazerolle, M. J.: AICcmodavg: Model selection and multimodel inference based on (Q)AIC(c) [code], 2023.

Meeran, K., Verbrigghe, N., Ingrisch, J., Fuchslueger, L., Müller, L., Sigurðsson, P., Sigurdsson, B. D., Wachter, H., Watzka, M., Soong, J. L., Vicca, S., Janssens, I. A., and Bahn, M.: Individual and interactive effects of warming and nitrogen supply on CO2 fluxes and carbon allocation in subarctic grassland, Global Change Biology, 29, 5276-5291, https://doi.org/10.1111/gcb.16851, 2023.

Melillo, J. M., Frey, S. D., DeAngelis, K. M., Werner, W. J., Bernard, M. J., Bowles, F. P., Pold, G., Knorr, M. A., and Grandy, A. S.: Long-term pattern and magnitude of soil carbon feedback to the climate system in a warming world, Science, 358, 101-105, 10.1126/science.aan2874, 2017.

Meyer, N., Welp, G., and Amelung, W.: The Temperature Sensitivity (Q10) of Soil Respiration: Controlling Factors and Spatial Prediction at Regional Scale Based on Environmental Soil Classes, Global Biogeochemical Cycles, 32, 306-323, https://doi.org/10.1002/2017GB005644, 2018.

Mortier, S., Hamedpour, A., Bussmann, B., Wandji, R. P. T., Latré, S., Sigurdsson, B. D., De Schepper, T., and Verdonck, T.: Inferring the relationship between soil temperature and the normalized difference vegetation index with machine learning, Ecological Informatics, 82, 102730, https://doi.org/10.1016/j.ecoinf.2024.102730, 2024.

https://doi.org/10.5194/egusphere-2026-4047
Preprint. Discussion started: 20 August 2026

Natali, S. M., Watts, J. D., Rogers, B. M., Potter, S., Ludwig, S. M., Selbmann, A.-K., Sullivan, P. F., Abbott, B. W., Arndt, K. A., Birch, L., Björkman, M. P., Bloom, A. A., Celis, G., Christensen, T. R., Christiansen, C. T., Commane, R., Cooper, E. J., Crill, P., Czimczik, C., Davydov, S., Du, J., Egan, J. E., Elberling, B., Euskirchen, E. S., Friborg, T., Genet, H., Göckede, M., Goodrich, J. P., Grogan, P., Helbig, M., Jafarov, E. E., Jastrow, J. D., Kalhori, A. A. M., Kim, Y., Kimball, J. S., Kutzbach, L., Lara, M. J., Larsen, K. S., Lee, B.-Y., Liu, Z., Loranty, M. M., Lund, M., Lupascu, M., Madani, N., Malhotra, A., Matamala, R., McFarland, J., McGuire, A. D., Michelsen, A., Minions, C., Oechel, W. C., Olefeldt, D., Parmentier, F.-J. W., Pirk, N., Poulter, B., Quinton, W., Rezanezhad, F., Risk, D., Sachs, T., Schaefer, K., Schmidt, N. M., Schuur, E. A. G., Semenchuk, P. R., Shaver, G., Sonnentag, O., Starr, G., Treat, C. C., Waldrop, M. P., Wang, Y., Welker, J., Wille, C., Xu, X., Zhang, Z., Zhuang, Q., and Zona, D.: Large loss of CO2 in winter observed across the northern permafrost region, Nature Climate Change, 9, 852-857, 10.1038/s41558-019-0592-8, 2019.

National Oceanic and Atmospheric Administration (NOAA) Global Monitoring Laboratory: Trends in Atmospheric CO_2, https://gml.noaa.gov/ccgg/trends/, last access: 17 April 2026.

Numa, K. B., Robinson, J. M., Arcus, V. L., and Schipper, L. A.: Separating the temperature response of soil respiration derived from soil organic matter and added labile carbon compounds, Geoderma, 400, 115128, https://doi.org/10.1016/j.geoderma.2021.115128, 2021.

O'Gorman, E. J., Chemshirova, I., McLaughlin, Ó. B., and Stewart, R. I.: Impacts of warming on reciprocal subsidies between aquatic and terrestrial ecosystems, Frontiers in Ecology and Evolution, 9, 795603, 2021.

Ogle, D. H., Doll, J. C., Wheeler, A. P., and Dinno, A.: FSA: Simple Fisheries Stock Assessment Methods [code], 2025.

Parkin, T. B. and Venterea, R. T.: USDA-ARS GRACEnet Project Protocols Chapter 3. Chamber-Based Trace Gas Flux Measurements 4, 2010.

Phillips, C. L., Bond-Lamberty, B., Desai, A. R., Lavoie, M., Risk, D., Tang, J., Todd-Brown, K., and Vargas, R.: The value of soil respiration measurements for interpreting and modeling terrestrial carbon cycling, Plant and Soil, 413, 1-25, 2017.

Poeplau, C., Sigurðsson, P., and Sigurdsson, B. D.: Depletion of soil carbon and aggregation after strong warming of a subarctic Andosol under forest and grassland cover, SOIL, 6, 115-129, 10.5194/soil-6-115-2020, 2020.

Poeplau, C., Kätterer, T., Leblans, N. I. W., and Sigurdsson, B. D.: Sensitivity of soil carbon fractions and their specific stabilization mechanisms to extreme soil warming in a subarctic grassland, Global Change Biology, 23, 1316-1327, https://doi.org/10.1111/gcb.13491, 2017.

Poeplau, C., Don, A., Six, J., Kaiser, M., Benbi, D., Chenu, C., Cotrufo, M. F., Derrien, D., Gioacchini, P., and Grand, S.: Isolating organic carbon fractions with varying turnover rates in temperate agricultural soils–A comprehensive method comparison, Soil Biology and Biochemistry, 125, 10-26, 2018.

Prommer, J., Walker, T. W. N., Wanek, W., Braun, J., Zezula, D., Hu, Y., Hofhansl, F., and Richter, A.: Increased microbial growth, biomass, and turnover drive soil organic carbon accumulation at higher plant diversity, Global Change Biology, 26, 669-681, https://doi.org/10.1111/gcb.14777, 2020.

https://doi.org/10.5194/egusphere-2026-4047
Preprint. Discussion started: 20 August 2026

Protti-Sánchez, F., Avila, L. M., Meeran, K., Ingrisch, J., Sigurðsson, P., Larsen, K. S., Sigurdsson, B. D., Janssens, I., and Bahn, M.: Soil Respiration Responses to Prolonged Warming Vary Seasonally in a Subarctic Grassland, Global Change Biology, 31, e70388, https://doi.org/10.1111/gcb.70388, 2025.

Pumpanen, J., Kolari, P., Ilvesniemi, H., Minkkinen, K., Vesala, T., Niinistö, S., Lohila, A., Larmola, T., Morero, M., and Pihlatie, M.: Comparison of different chamber techniques for measuring soil CO2 efflux, Agricultural and Forest Meteorology, 123, 159-176, 2004.

Qu, L., Wang, C., Manzoni, S., Dacal, M., Maestre, F. T., and Bai, E.: Stronger compensatory thermal adaptation of soil microbial respiration with higher substrate availability, The ISME Journal, 18, wrae025, 10.1093/ismejo/wrae025, 2024.

Radujković, D., Verbruggen, E., Sigurdsson, B. D., Leblans, N. I. W., Janssens, I. A., Vicca, S., and Weedon, J. T.: Prolonged exposure does not increase soil microbial community compositional response to warming along geothermal gradients, FEMS Microbiology Ecology, 94, fix174, 10.1093/femsec/fix174, 2018.

Robinson, J. M., O'Neill, T. A., Ryburn, J., Liang, L. L., Arcus, V. L., and Schipper, L. A.: Rapid laboratory measurement of the temperature dependence of soil respiration and application to changes in three diverse soils through the year, Biogeochemistry, 133, 101-112, 10.1007/s10533-017-0314-0, 2017.

Sadatshojaei, E., Wood, D. A., and Rahimpour, M. R.: Potential and Challenges of Carbon Sequestration in Soils, in: Applied Soil Chemistry, 1-21, https://doi.org/10.1002/9781119711520.ch1, 2021.

Sampath, V., Shalakhti, O., Veidis, E., Efobi, J. A. I., Shamji, M. H., Agache, I., Skevaki, C., Renz, H., and Nadeau, K. C.: Acute and chronic impacts of heat stress on planetary health, Allergy, 78, 2109-2120, https://doi.org/10.1111/all.15702, 2023.

Schwarz, E., Ghersheen, S., Belyazid, S., and Manzoni, S.: When and why microbial-explicit soil organic carbon models can be unstable, Biogeosciences, 21, 3441-3461, 10.5194/bg-21-3441-2024, 2024.

Scott, S. W., Lévy, L., Covell, C., Franzson, H., Gibert, B., Valfells, Á., Newson, J., Frolova, J., Júlíusson, E., and Guðjónsdóttir, M. S.: Valgarður: a database of the petrophysical, mineralogical, and chemical properties of Icelandic rocks, Earth Syst. Sci. Data, 15, 1165-1195, 10.5194/essd-15-1165-2023, 2023.

Shimada, H., Wagai, R., Inoue, Y., Tamura, K., and Asano, M.: Millennium timescale carbon stability in an Andisol: How persistent are organo-metal complexes?, Geoderma, 417, 115820, https://doi.org/10.1016/j.geoderma.2022.115820, 2022.

Sigurdsson, B. D., Leblans, N. I., Dauwe, S., Gudmundsdottir, E., Gundersen, P., Gunnarsdottir, G. E., Holmstrup, M., Ilieva-Makulec, K., Katterer, T., and Marteinsdottir, B.-S.: Geothermal ecosystems as natural climate change experiments: The ForHot research site in Iceland as a case study, Icelandic agricultural sciences.-Reykjavik, Akureyri, 29, 53-71, 2016.

Smith, D. L. and Johnson, L.: Vegetation-mediated changes in microclimate reduce soil respiration as woodlands expand into grasslands, Ecology, 85, 3348-3361, 2004.

Söllinger, A., Ahlers, L. S., Dahl, M. B., Sigurðsson, P., Le Noir de Carlan, C., Bhattarai, B., Gall, C., Martin, V. S., Rottensteiner, C., and Motleleng, L. L.: Microorganisms in subarctic soils are depleted of ribosomes under short-, medium-, and long-term warming, The ISME Journal, 18, wrae081, 2024.

https://doi.org/10.5194/egusphere-2026-4047
Preprint. Discussion started: 20 August 2026

Sun, H., Li, J., Liu, H., Fang, C., Li, B., and Nie, M.: Global change factors regulate the apparent thermal acclimation of soil respiration: A meta-analysis, Applied Soil Ecology, 183, 104741, https://doi.org/10.1016/j.apsoil.2022.104741, 2023.

Sun, Y., Jiang, S., Zhou, Y., Zou, X., and Chen, X.: Critical Thresholds of Warming Magnitude, Duration, and Soil Depth Control Soil Carbon Vulnerability, Ecosystems, 28, 1-9, 2025.

Tao, X., Yang, Z., Feng, J., Jian, S., Yang, Y., Bates, C. T., Wang, G., Guo, X., Ning, D., Kempher, M. L., Liu, X. J. A., Ouyang, Y., Han, S., Wu, L., Zeng, Y., Kuang, J., Zhang, Y., Zhou, X., Shi, Z., Qin, W., Wang, J., Firestone, M. K., Tiedje, J. M., and Zhou, J.: Experimental warming accelerates positive soil priming in a temperate grassland ecosystem, Nature Communications, 15, 1178, 10.1038/s41467-024-45277-0, 2024.

Taseski, G. M., Keith, D. A., Dalrymple, R. L., and Cornwell, W. K.: Shifts in fine root traits within and among species along a fine-scale hydrological gradient, Annals of Botany, 127, 473-481, 10.1093/aob/mcaa175, 2021.

Team, R. C.: R: A Language and Environment for Statistical Computing, R Foundation for Statistical Computing [code], 2025.

Thien, B. M. J., Kosakowski, G., and Kulik, D. A.: Differential alteration of basaltic lava flows and hyaloclastites in Icelandic hydrothermal systems, Geothermal Energy, 3, 11, 10.1186/s40517-015-0031-7, 2015.

Toms, J. D. and Lesperance, M. L.: Piecewise Regression: A Tool for Identifying Ecological Thresholds, Ecology, 84, 2034-2041, 2003.

Torn, M. S., Abramoff, R. Z., Vaughn, L. J. S., Chafe, O. E., Curtis, J. B., and Zhu, B.: Large emissions of CO2 and CH4 due to active-layer warming in Arctic tundra, Nature Communications, 16, 124, 10.1038/s41467-024-54990-9, 2025.

Tucker, C. L., Bell, J., Pendall, E., and Ogle, K.: Does declining carbon-use efficiency explain thermal acclimation of soil respiration with warming?, Global Change Biology, 19, 252-263, https://doi.org/10.1111/gcb.12036, 2013.

Ťupek, B., Lehtonen, A., Manzoni, S., Bruni, E., Baldrian, P., Richy, E., Adamczyk, B., Guenet, B., and Mäkipää, R.: Reduced microbial respiration sensitivity to soil moisture following long-term N fertilization enhances soil C retention in a boreal Scots pine forest, EGUsphere, 2024, 1-23, 10.5194/egusphere-2024-3813, 2024.

Van't Hoff, J. H. and Lehfeldt, R. A.: Lectures on theoretical and physical chemistry, 1900.

Verbrigghe, N., Leblans, N. I. W., Sigurdsson, B. D., Vicca, S., Fang, C., Fuchslueger, L., Soong, J. L., Weedon, J. T., Poeplau, C., Ariza-Carricondo, C., Bahn, M., Guenet, B., Gundersen, P., Gunnarsdóttir, G. E., Kätterer, T., Liu, Z., Maljanen, M., Marañón-Jiménez, S., Meeran, K., Oddsdóttir, E. S., Ostonen, I., Peñuelas, J., Richter, A., Sardans, J., Sigurðsson, P., Torn, M. S., Van Bodegom, P. M., Verbruggen, E., Walker, T. W. N., Wallander, H., and Janssens, I. A.: Soil carbon loss in warmed subarctic grasslands is rapid and restricted to topsoil, Biogeosciences, 19, 3381-3393, 10.5194/bg-19-3381-2022, 2022.

Vicca, S., Bahn, M., Estiarte, M., van Loon, E. E., Vargas, R., Alberti, G., Ambus, P., Arain, M. A., Beier, C., Bentley, L. P., Borken, W., Buchmann, N., Collins, S. L., de Dato, G., Dukes, J. S., Escolar, C., Fay, P., Guidolotti, G., Hanson, P. J., Kahmen, A., Kröel-Dulay, G., Ladreiter-Knauss, T., Larsen, K. S., Lellei-Kovacs, E., Lebrija-Trejos, E., Maestre, F. T., Marhan, S., Marshall, M., Meir, P., Miao, Y., Muhr, J., Niklaus, P. A., Ogaya, R., Peñuelas, J., Poll, C., Rustad, L. E., Savage, K., Schindlbacher, A., Schmidt, I. K., Smith, A. R., Sotta, E. D., Suseela, V., Tietema, A., van Gestel, N., van

https://doi.org/10.5194/egusphere-2026-4047
Preprint. Discussion started: 20 August 2026

Straaten, O., Wan, S., Weber, U., and Janssens, I. A.: Can current moisture responses predict soil CO₂ efflux under altered precipitation regimes? A synthesis of manipulation experiments, Biogeosciences, 11, 2991-3013, 10.5194/bg-11-2991-2014, 2014.

von Lützow, M. and Kögel-Knabner, I.: Temperature sensitivity of soil organic matter decomposition-what do we know?, BIOLOGY AND FERTILITY OF SOILS, 46, 1-15, 10.1007/s00374-009-0413-8, 2009.

Walker, T. W. N., Kaiser, C., Strasser, F., Herbold, C. W., Leblans, N. I. W., Woebken, D., Janssens, I. A., Sigurdsson, B. D., and Richter, A.: Microbial temperature sensitivity and biomass change explain soil carbon loss with warming, Nature Climate Change, 8, 885-889, 10.1038/s41558-018-0259-x, 2018.

Wang, C., Morrissey, E. M., Mau, R. L., Hayer, M., Piñeiro, J., Mack, M. C., Marks, J. C., Bell, S. L., Miller, S. N., Schwartz, E., Dijkstra, P., Koch, B. J., Stone, B. W., Purcell, A. M., Blazewicz, S. J., Hofmockel, K. S., Pett-Ridge, J., and Hungate, B. A.: The temperature sensitivity of soil: microbial biodiversity, growth, and carbon mineralization, The ISME Journal, 15, 2738-2747, 10.1038/s41396-021-00959-1, 2021.

Wasner, D., Walker, T. W., Bektaş, B., Network, T., and Alexander, J. M.: Rapid acclimation of topsoil physicochemical and biotic properties to experimental climate change, EGU General Assembly Conference Abstracts, EGU25-12202,

Weedon, J. T., Bååth, E., Rijkers, R., Reischke, S., Sigurdsson, B. D., Oddsdottir, E., van Hal, J., Aerts, R., Janssens, I. A., and van Bodegom, P. M.: Community adaptation to temperature explains abrupt soil bacterial community shift along a geothermal gradient on Iceland, Soil Biology and Biochemistry, 177, 108914, https://doi.org/10.1016/j.soilbio.2022.108914, 2023.

Wieder, W. R., Bonan, G. B., and Allison, S. D.: Global soil carbon projections are improved by modelling microbial processes, Nature Climate Change, 3, 909-912, 10.1038/nclimate1951, 2013.

Wu, Q., Ye, R., Bridgham, S. D., and Jin, Q.: Limitations of the Q10 Coefficient for Quantifying Temperature Sensitivity of Anaerobic Organic Matter Decomposition: A Modeling Based Assessment, Journal of Geophysical Research: Biogeosciences, 126, e2021JG006264, https://doi.org/10.1029/2021JG006264, 2021.

Zhang, Q., Feng, J., Li, X., Chen, Y., Schimel, J. P., and Zhu, B.: Effect of field warming on soil microbial carbon use efficiency——A meta-analysis, Soil Biology and Biochemistry, 197, 109531, https://doi.org/10.1016/j.soilbio.2024.109531, 2024.

Ziegler, S. E., Benner, R., Billings, S. A., Edwards, K. A., Philben, M., Zhu, X., and Laganière, J.: Climate Warming Can Accelerate Carbon Fluxes without Changing Soil Carbon Stocks, Frontiers in Earth Science, 5, 10.3389/feart.2017.00002, 2017.